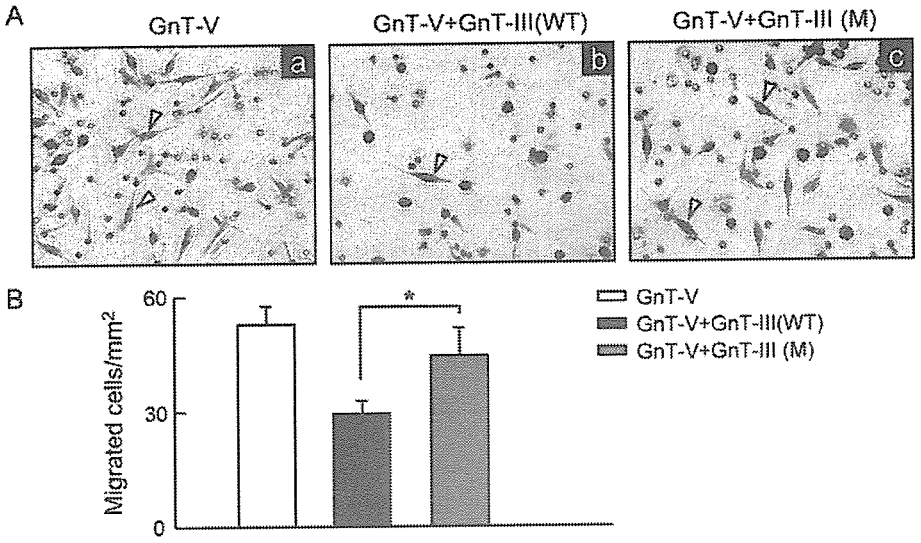

FIGURE 3. **GnT-III transfection suppressed cell migration stimulated by GnT-V.** *A*, cells were replated on the upper chamber coated with LN5 (5 nM). Cell migration was investigated by the GnT-V transfectant (*a*), GnT-III transfection to GnT-V transfectant (*b*), and GnT-III mutant transfection to GnT-V transfectant (*c*). Representative fields were photographed using a phase-contrast microscope. The *arrowheads* indicate migrated cells. *B*, the numbers of migrated cells were quantified and expressed as the means ± S.D. from three independent experiments. *WT*, wild type.

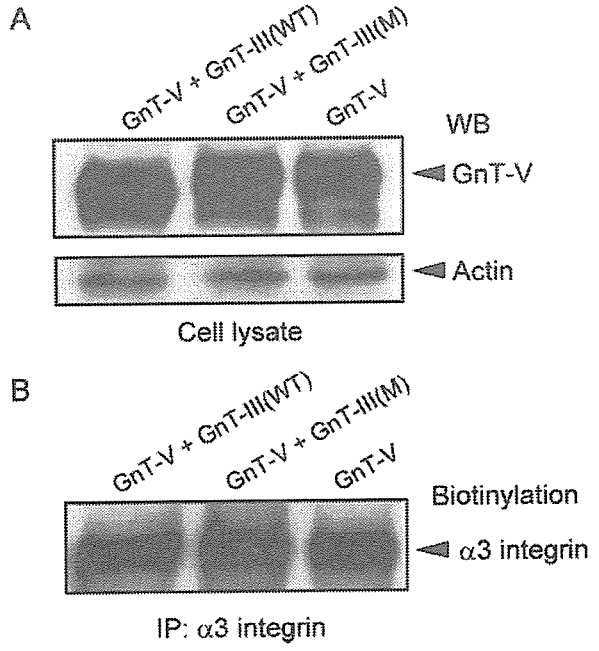

FIGURE 4. **No effects of GnT-III transfection on expression levels of both GnT-V and integrin α3 subunit expressed on cell surface.** *A*, double-transfected cells were lysed, and whole lysates were subjected to 7.5% SDS-PAGE and then transferred to a nitrocellulose membrane and blotted with GnT-V antibody (*top*) or actin antibody (*bottom*). *B*, transfected cells were biotinylated, whole lysates were immunoprecipitated (*IP*) with anti-α3 antibody, and the samples were subjected to 7.5% SDS-PAGE and transferred to a nitrocellulose membrane. The biotinylated proteins were then detected as described under "Experimental Procedures." *WT*, wild type; *WB*, Western blot.

the expression of glycoproteins. As shown in Fig. 4*A*, the levels of expression of GnT-V were not influenced by the introduction of GnT-III, and equivalent amounts of loaded proteins were verified by blotting an actin antibody. On the other hand, the expression of integrin α3 subunit on the cell surface also remained unchanged among the transfectants of GnT-III plus GnT-V, GnT-III mutant plus GnT-V, and GnT-V (Fig. 4*B*). These results suggested that the inhibition of GnT-III- to GnT-V-induced cell migration could not be ascribed to a change in the expression levels of GnT-V and/or α3 subunit on the cell surface.

Transfection of GnT-III Had No Effect on the Activity of GnT-V—Since the introduction of GnT-III had no effect on the expressions of GnT-V and α3 subunit, we further determined if the overexpression of GnT-III suppressed the activity of GnT-V. Since this was a transient transfection, the activity of GnT-III was checked at six time points from 24 to 144 h after the transfection. We found that GnT-III activity reached the highest level 48 h after transfection (Fig. 5*A*), and there was no corresponding activity in GnT-III mutant (data not shown). The expression level of GnT-III mutant was similar to that of wild-type GnT-III confirmed by blotting with GnT-III antibody, and equivalent amounts of loaded proteins were verified by blotting with anti-actin antibody (Fig. 5*B*). As shown in Fig. 5*C*, GnT-V activity was found to be stable, even in the period (48 h after transfection) where the activity of GnT-III reached the highest level in these double-transfected cells. This result indicated that GnT-III inhibited GnT-V-induced cell migration not due to the suppression of GnT-V activity.

Increased GnT-III Product but Decreased GnT-V Product on Integrin α3 Subunit—The modification of *N*-glycosylation contributes to the functions of integrins (39). Here, we checked whether changes of α3β1 integrin modification had occurred in these transfectants. The integrins were immunoprecipitated from these transfectants and then probed with E_4-PHA lectin, which preferentially binds to bisecting GlcNAc residues in *N*-glycans, or L_4-PHA lectin, which binds to β1,6-branched GlcNAc. Fig. 6*A* (*top*) shows that the transfection of GnT-III to the GnT-V transfectant resulted in an increase in the GnT-III product on the integrin α3 subunit. More interestingly, the level of GnT-V product on α3 was decreased in the double transfectants (Fig. 6*A*, *middle*). Consistent with this observation, transfection of the GnT-III mutant failed to induce such changes. Equivalent amounts of the α3 subunit were verified by blotting α3-immunoprecipitated lysates (Fig. 6*A*, *bottom*). Moreover, cell lysates were subjected to SDS-PAGE, followed by a lectin blot. A comparison of bands especially around 117–200 and 60–89 kDa among these transfectants consistently indicated that increased GnT-III products but decreased GnT-V products presented on the glycoproteins after the introduction of GnT-III to the GnT-V transfectant (Fig. 6*B*). Furthermore, to further confirm such competition on the α3 sub-

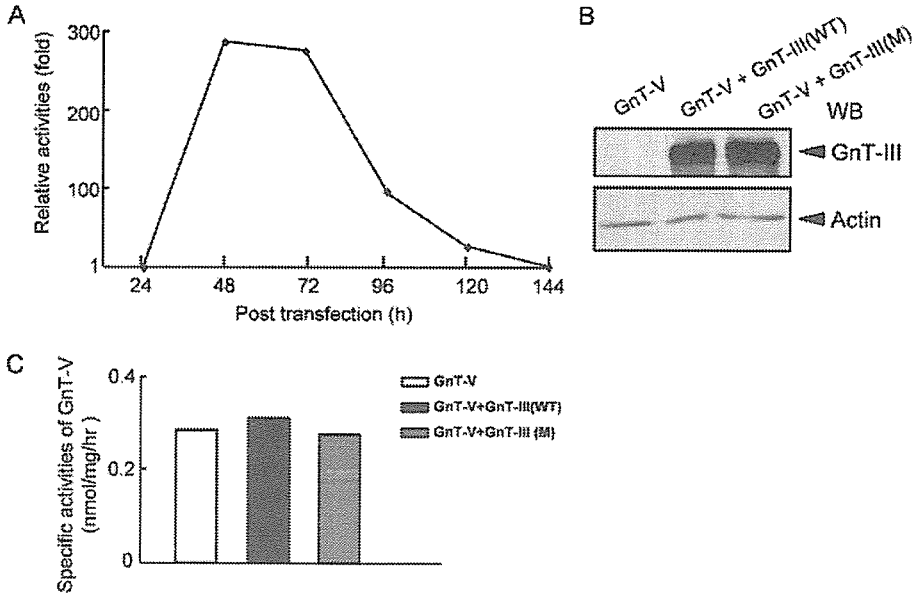

FIGURE 5. **No effects of GnT-III transfection on activity of GnT-V.** *A*, GnT-III activity of transient transfection of adenoviral expression vector to the GnT-V transfectant was examined by high performance liquid chromatography using a fluorescence-labeled agalactobiantennary sugar chain as a substrate. GnT-III activity was determined at various time points (6 days). Data are expressed as a ratio to the first time point (24 h after transfection). *B*, double-transfected cells were lysed, and whole lysates were subjected to 7.5% SDS-PAGE and then transferred to a nitrocellulose membrane and blotted with GnT-III antibody (*top*) or actin antibody (*bottom*). *C*, GnT-V activity of the transient transfection of the adenoviral expression vector to GnT-V transfectant was investigated using the method mentioned in *A* at the time point of 48 h after transfection. Data are expressed as specific activity (nmol of product/mg of lysate/h). *WT*, wild type; *WB*, Western blot.

unit, we purified this integrin from GnT-III, GnT-V, and GnT-III plus GnT-V transfectants using a GD6 peptide affinity column combined with a wheat germ agglutinin affinity column. The purity was evaluated by SDS-PAGE followed by silver staining (data not shown). The purified α3 subunit was cut from gels and then subjected to LC/MS^n as described under "Experimental Procedures." As shown in Fig. 6, *C* and *D*, mass spectra of desialylated *N*-glycans were obtained from the α3 expressed in GnT-III, GnT-V, and GnT-III plus GnT-V transfectants, respectively, by a full MS1 scan (*m/z* 450–2000). Carbohydrate structures of the major peaks were deduced from the *m/z* values of protonated ions in the full MS^1 spectra obtained by FT-ICR MS and product ions in MS^{2,3} spectra (Fig. 6*D*). Based on the presence of $[HexNAc\text{-}Hex\text{-}HexNAc\text{-}HexNAc\text{-}OH + H]^+$ (*m/z* 792) and $[HexNAc\text{-}Hex\text{-}HexNAc\text{-}(dHex)HexNAc\text{-}OH + H]^+$ (*m/z* 938) in MS2,3 spectra, peaks 4, 5, 7, 8, 10, and 11 were determined as bisected glycans. Peak 4 was deduced to be a biantennary oligosaccharide, the major peak in the GnT-III transfectant. After the transfection of GnT-III into the GnT-V transfectant, peak 4 was increased compared with that of the GnT-V transfectant, whereas peak 6, which is the major peak in the GnT-V transfectant, was decreased. For the present technique, the branched form is determined by analyzing the sialylated oligosaccharides by LC/MS^n in the negative ion mode. Referring to the result of the L_4-PHA lectin blot and the fact that peak 6 is the major one in the GnT-V transfectant, peak 6 could be deduced the β1,6-branched GlcNAc form, although only bisialylated forms were detected by MS. The MS data also revealed that peaks 7 or 8 and 9, 10, or 11 were triantennary and tetraantennary oligosaccharides, respectively, from the presence of their corresponding trisialylated and tetrasialylated forms. Peaks 1 and 2 were high mannose oligosaccharides. To further quantify the competition, we used the MS results to show that for GnT-III products (represented by the sum of the peaks 4, 5, 7, 8, 10, and 11), the proportion was, respectively, 79.5, 29.5, and 48.5% among the transfectants of GnT-III, GnT-V, and GnT-III plus GnT-V; for GnT-V products (represented by the sum of peaks 6 and 9), the proportion was 1.2, 34.9, and 18.1%, respectively, among the transfectants of GnT-III, GnT-V, and GnT-III plus GnT-V. Consistent with the results shown in Fig. 6*A*, these data strongly suggested that GnT-III transfection resulted in increased bisecting GlcNAc but decreased β1,6-branched GlcNAc on the α3 subunit. However, the *N*-glycan proportions partially, but not totally, are correlated with the extent of the modification in cell migration observed (Fig. 3), since only *N*-glycans located on some motifs of integrins have been proposed to influence their conformations and therefore to regulate their functions (40).[4] Taken together, these results suggested the following; α3 was a common target of GnT-III and GnT-V, and the priority taken by GnT-III in the competition resulted in the inhibition of GnT-V modification.

Increased β1,6-Branched GlcNAc as Well as Cell Migration in GnT-III Knockdown Cells—To further identify the competition of GnT-III and GnT-V definitely, we developed an RNA interference strategy to efficiently silence GnT-III expression in CHP134 cells, which express endogenous GnT-III and GnT-V. After retroviral infection, CHP134 cells were selected based on their resistance to G418 as described under "Experimental Procedures." GnT-III activity was effectively down-regulated by 70%, compared with those in parent and mock cells (Fig. 7*A*), whereas GnT-V activity, as a control, showed no significant changes (data not shown). A quantitative real time PCR analysis also indicated the down-regulation of RNA interference-directed GnT-III mRNA expression in these cells (Fig. 7*B*). We then tested cell migration on LN5 and found that GnT-III knockdown resulted in an increased cell migration compared with mock cells (Fig. 7, *C* and *D*). We further investigated the *N*-glycans on the α3 subunit. As shown in Fig. 7*E*, increased β1,6-branched GlcNAc but decreased bisecting GlcNAc on α3 was found in the GnT-III knockdown cells, compared with those in the mock cells. Together with the data in Fig. 6, these data provided the evidence to show that GnT-III inhibited

[4] Isaji, T., Sato, Y., Zhao, Y., Miyoshi, E., Wada, Y., Taniguchi, N., and Gu, J. (2006) *J. Biol. Chem.*, in press.

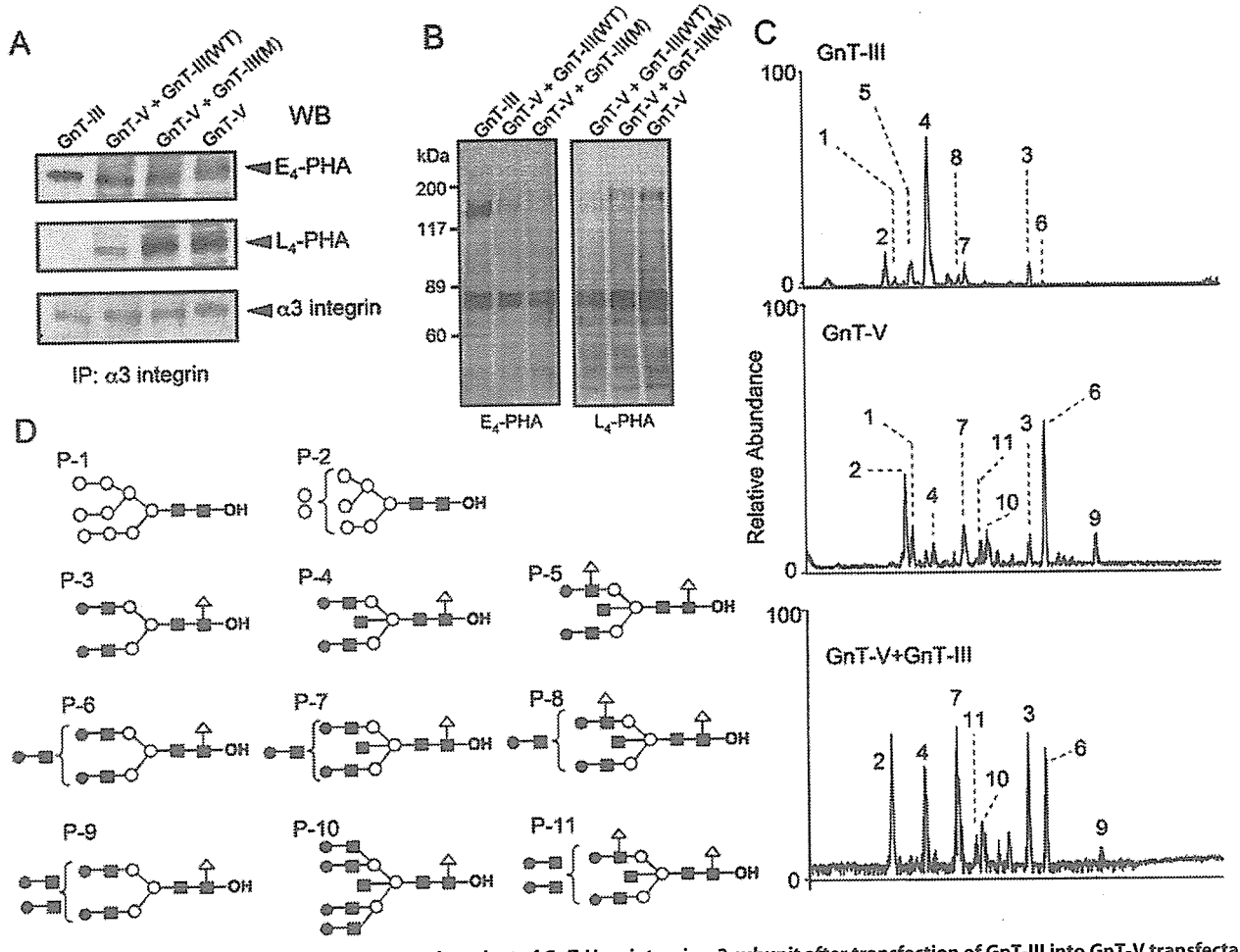

FIGURE 6. **Increased product of GnT-III but decreased product of GnT-V on integrin α3 subunit after transfection of GnT-III into GnT-V transfectant.** *A*, whole cell lysates were immunoprecipitated (*IP*) with anti-α3 antibody, and the resulting immunocomplexes were subjected to 7.5% SDS-PAGE under reducing conditions. The blots were probed by E_4-PHA (*top*), L_4-PHA (*middle*) and anti-α3 antibody (*bottom*), respectively. *B*, lectin blotting was performed with E_4-PHA and L_4-PHA using cell lysates from different transfectants. *C*, base peak chromatograms and observed *m/z* values (charge number) obtained by a full MS1 scan (*m/z* 450–2000) of *N*-linked oligosaccharides extracted from the gel-separated α3 subunit expressed in transfectants: GnT-III transfectant (*top*), GnT-V transfectant (*middle*), and GnT-III plus GnT-V transfectant (*bottom*). *D*, deduced structures of peaks 1–11. △, fucose; ●, galactose; ○, mannose; ■, *N*-acetylglucosamine. *WB*, Western blot.

the functions of GnT-V by competing for the modification of the same protein in living cells, resulting in the positive or negative regulation of its biological functions.

DISCUSSION

It has long been thought that the product of GnT-V, β1,6-GlcNAc branching of *N*-glycans, contributes directly to cancer progression and metastasis (6). Animal studies have shown that GnT-V-deficient transgenic mice experience attenuated tumor growth and metastasis (3). In human, the activity and/or expression of GnT-V is elevated in multiple types of tumors (41, 42), and high levels of these enzymes or their cognate sugars are correlated with metastasis and a poor patient prognosis (41, 43). In addition, GnT-V-modified cell surface receptors prolonged the turnover by inhibiting endocytosis (10) or resistance to degradation by protease (26). These results suggest that GnT-V may contribute to cancer metastasis through stabilizing target proteins. On the other hand, the introduction of GnT-III leads to a reduced metastatic potential. Moreover, those transfectants displayed decreased cell motility and attachment to laminin and collagen (14). Thus, it appears that GnT-V and GnT-III regulate cell migration and invasion as well as metastasis in opposite manners. In fact, GnT-III could be considered to be an antagonist of GnT-V, because bisecting GlcNAc renders the biantennary substrate inaccessible to GnT-V *in vitro* (13).

The α3β1 integrin is one of the most important proteins that mediate cell motility and invasion and appears to be one of the plausible target proteins of GnT-V in promoting cancer metastasis. In fact, Pochec *et al.* (25) reported that β1,6-branched structures were highly expressed in high metastatic melanoma, compared with low metastatic melanoma. In the present study, we found for the first time that GnT-III and GnT-V competitively modify the same target, integrin α3 subunit, thereby regulating its functions. We demonstrated that GnT-III transfection to the GnT-V transfectant resulted in the inhibition of α3β1 integrin-mediated cell migration, due to an increase of

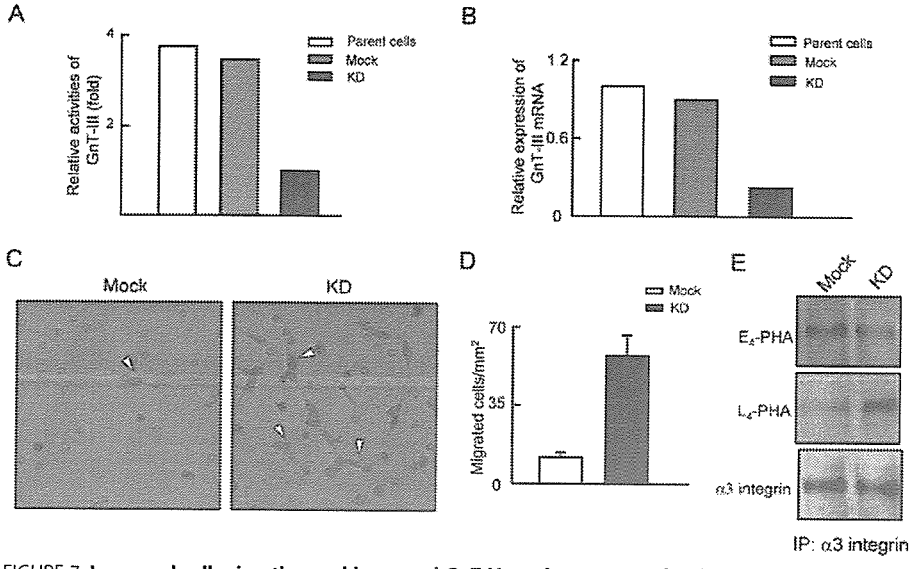

FIGURE 7. **Increased cell migration and increased GnT-V product on α3 subunit in GnT-III knockdown cells.** *A*, activities of GnT-III in GnT-III knockdown CHP134 cells. *B*, mRNA expression of GnT-III in knockdown cells. Quantitative analysis was performed by real time PCR. *C*, cell migration on LN5 (5 nM). Representative fields were photographed using a phase-contrast microscope. *Arrowheads*, migrated cells. *D*, quantification of migration of mock and GnT-III knockdown cells. The number of migrated cells were quantified and expressed as the means ± S.D. from three independent experiments. *E*, whole cell lysates were immunoprecipitated (*IP*) with anti-α3 antibody, and the resulting immunocomplexes were subjected to 7.5% SDS-PAGE under reducing condition. The blots were probed by E_4-PHA (*top*), L_4-PHA (*middle*), and anti-α3 antibody (*bottom*), respectively. *KD*, GnT-III knockdown cells.

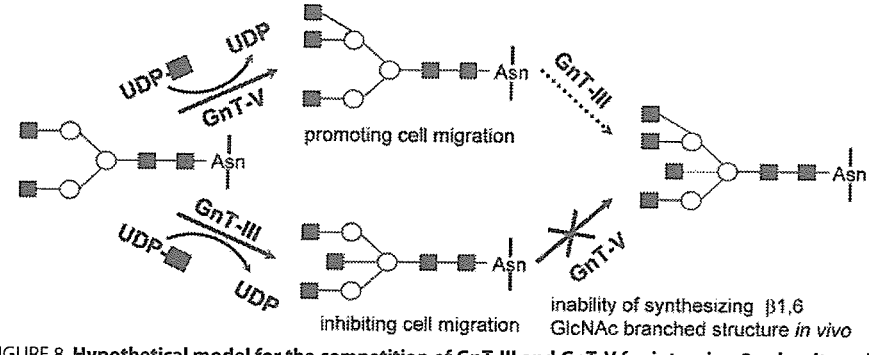

FIGURE 8. **Hypothetical model for the competition of GnT-III and GnT-V for integrin α3 subunit modification.** The product of GnT-V contributes to the promotion of cell migration. The reaction represented by a *dashed line* may not be predominant *in vivo*, whereas it could occur *in vitro*. On the other hand, the product of GnT-III suppresses cell migration. More importantly, this product cannot be utilized as a substrate by GnT-V, which is represented with a *cross*. Therefore, α3β1-mediated cell migration induced by GnT-V can be blocked due to competition with GnT-III. ○, mannose; ■, *N*-acetylglucosamine.

bisecting GlcNAc, but a decreased β1,6-GlcNAc, on the α3 subunit. However, the transfection of the GnT-III inactive mutant failed to induce such changes. Conversely, the competition was further confirmed by an RNA interference strategy to silence GnT-III in CHP134 cells, which express endogenous GnT-V and GnT-III. We found that GnT-III knockdown resulted in increased GnT-V product on the α3 subunit. Taken together, to the best of our knowledge, we presented a previously uncharacterized demonstration of the existence of competition for the same substrate between GnT-III and GnT-V in living cells (Fig. 8).

Two mechanisms have been proposed for the inhibition of cell motility by the overexpression of GnT-III: an enhancement in cell-cell adhesion and the down-regulation of cell-ECM adhesion (39). Our present study suggested one more; GnT-III competed with GnT-V for the modification of α3 subunit, causing a decrease in the product of GnT-V on α3 subunit. Luo *et al.* (40) had suggested that the changes in the glycan structure of integrin can affect its conformation and activity. They reported that in CHO-K1 cells, the addition of a glycan at the β1 I-like domain caused an increase in the distance between the β1 head and stalk domains, therefore inducing the integrin dimer to be a more extended (activated) integrin conformation (40). We suggested that the competition of GnT-III and GnT-V for the modification of α3 may cause changes in the glycan within key regions of this integrin, therefore causing the decreased cell migration. Details of the effect of glycans on this integrin are a subject of further investigation in our future study.

It is noteworthy that GnT-III and GnT-V do not always oppositely regulate all glycoproteins. In this study, we found that GnT-III transfection causes a similar decrease, but to a lesser extent, in cell migration on COL compared with the result on LN5. However, on COL, GnT-V transfection did not result in an increase in cell migration, compared with mock. This suggested that β1,6-GlcNAc modification has little effect or only mild effects on α1β1 and α2β1 integrin, which are receptors for COL. In fact, we reported that the introduction of the bisecting GlcNAc to the α5 subunit resulted in a reduced affinity in the binding of α5β1 integrin to FN, resulting in a decreased cell migration (38). We thus assumed that the GnT-III affects the α1, α2, and α3 subunits similarly, which caused the decreased cell migration on LN5 and COL. However, the modification of β1,6-GlcNAc to α1 and α2 subunits may not affect their binding to COL. Considering that α3β1 integrin is a strong adhesive receptor that promotes cell migration (37), the selective competition between GnT-III and GnT-V for α3 might play an important role in cancer metastasis.

Concerning metastasis, other important glycosyltransferases cannot be overlooked (*e.g.* sialyltransferases). The modification of the β1 subunit by sialyltransferase makes this integrin capped with the negatively charged sugar, sialic acid. The abundance of sialic acids, especially elevated α2,6-sialylation (44), contributes

to cell motility and invasion (25, 45–47). Thus, it is possible that GnT-V mediates at least some of its effects on cell behavior via increased sialylation (41). The effect of GnT-III on sialylation is a topic that also merits further exploration.

In conclusion, this study reports for the first time that GnT-III competes with GnT-V for the modification of integrin α3 subunit in living cells (Fig. 8). This competition results in the inhibition of α3β1 integrin-mediated cell migration induced by GnT-V. The finding suggests that the competition between both enzymes occurs not only *in vitro* but also *in vivo* and might provide a new insight into unraveling the molecular mechanism of tumor metastasis.

REFERENCES

1. Yamashita, K., Totani, K., Iwaki, Y., Kuroki, M., Matsuoka, Y., Endo, T., and Kobata, A. (1989) *J. Biol. Chem.* **264,** 17873–17881
2. Pierce, M., and Arango, J. (1986) *J. Biol. Chem.* **261,** 10772–10777
3. Granovsky, M., Fata, J., Pawling, J., Muller, W. J., Khokha, R., and Dennis, J. W. (2000) *Nat. Med.* **6,** 306–312
4. Cummings, R. D., Trowbridge, I. S., and Kornfeld, S. (1982) *J. Biol. Chem.* **257,** 13421–13427
5. Shoreibah, M., Perng, G. S., Adler, B., Weinstein, J., Basu, R., Cupples, R., Wen, D., Browne, J. K., Buckhaults, P., and Fregien, N. (1993) *J. Biol. Chem.* **268,** 15381–15385
6. Dennis, J. W., Laferte, S., Waghorne, C., Breitman, M. L., and Kerbel, R. S. (1987) *Science* **236,** 582–585
7. Demetriou, M., Nabi, I. R., Coppolino, M., Dedhar, S., and Dennis, J. W. (1995) *J. Cell Biol.* **130,** 383–392
8. Seberger, P. J., and Chaney, W. G. (1999) *Glycobiology* **9,** 235–241
9. Lu, Y., Pelling, J. C., and Chaney, W. G. (1994) *Clin. Exp. Metastasis* **12,** 47–54
10. Partridge, E. A., Le Roy, C., Di Guglielmo, G. M., Pawling, J., Cheung, P., Granovsky, M., Nabi, I. R., Wrana, J. L., and Dennis, J. W. (2004) *Science* **306,** 120–124
11. Narasimhan, S. (1982) *J. Biol. Chem.* **257,** 10235–10242
12. Schachter, H. (1986) *Biochem. Cell Biol.* **64,** 163–181
13. Gu, J., Nishikawa, A., Tsuruoka, N., Ohno, M., Yamaguchi, N., Kangawa, K., and Taniguchi, N. (1993) *J. Biochem. (Tokyo)* **113,** 614–619
14. Yoshimura, M., Nishikawa, A., Ihara, Y., Taniguchi, S., and Taniguchi, N. (1995) *Proc. Natl. Acad. Sci. U. S. A.* **92,** 8754–8758
15. Takeichi, M. (1993) *Curr. Opin. Cell Biol.* **5,** 806–811
16. Hirohashi, S. (1998) *Am. J. Pathol.* **153,** 333–339
17. Yoshimura, M., Ihara, Y., Matsuzawa, Y., and Taniguchi, N. (1996) *J. Biol. Chem.* **271,** 13811–13815
18. Hynes, R. O. (2002) *Cell* **110,** 673–687
19. Tsuji, T., Kawada, Y., Kai-Murozono, M., Komatsu, S., Han, S. A., Takeuchi, K., Mizushima, H., Miyazaki, K., and Irimura, T. (2002) *Clin. Exp. Metastasis* **19,** 127–134
20. Plopper, G. E., Domanico, S. Z., Cirulli, V., Kiosses, W. B., and Quaranta, V. (1998) *Breast Cancer Res. Treat.* **51,** 57–69
21. Melchiori, A., Mortarini, R., Carlone, S., Marchisio, P. C., Anichini, A., Noonan, D. M., and Albini, A. (1995) *Exp. Cell Res.* **219,** 233–242
22. Tysnes, B. B., Larsen, L. F., Ness, G. O., Mahesparan, R., Edvardsen, K., Garcia-Cabrera, I., and Bjerkvig, R. (1996) *Int. J. Cancer* **67,** 777–784
23. Wang, H., Fu, W., Im, J. H., Zhou, Z., Santoro, S. A., Iyer, V., DiPersio, C. M., Yu, Q. C., Quaranta, V., Al-Mehdi, A., and Muschel, R. J. (2004) *J. Cell Biol.* **164,** 935–941
24. Guo, H. B., Lee, I., Kamar, M., Akiyama, S. K., and Pierce, M. (2002) *Cancer Res.* **62,** 6837–6845
25. Pochec, E., Litynska, A., Amoresano, A., and Casbarra, A. (2003) *Biochim. Biophys. Acta* **1643,** 113–123
26. Ihara, S., Miyoshi, E., Ko, J. H., Murata, K., Nakahara, S., Honke, K., Dickson, R. B., Lin, C. Y., and Taniguchi, N. (2002) *J. Biol. Chem.* **277,** 16960–16967
27. Saito, H., Nishikawa, A., Gu, J., Ihara, Y., Soejima, H., Wada, Y., Sekiya, C., Niikawa, N., and Taniguchi, N. (1994) *Biochem. Biophys. Res. Commun.* **198,** 318–327
28. Miwa, K., Matsui, K., Terabe, M., Ito, K., Ishida, M., Takagi, H., Nakamori, S., and Sano, K. (1985) *Gene (Amst.)* **39,** 281–286
29. Taniguchi, N., Nishikawa, A., Fujii, S., and Gu, J. G. (1989) *Methods Enzymol.* **179,** 397–408
30. Nishikawa, A., Gu, J., Fujii, S., and Taniguchi, N. (1990) *Biochim. Biophys. Acta* **1035,** 313–318
31. Sato, Y., Takahashi, M., Shibukawa, Y., Jain, S. K., Hamaoka, R., Miyagawa, J., Yaginuma, Y., Honke, K., Ishikawa, M., and Taniguchi, N. (2001) *J. Biol. Chem.* **276,** 11956–11962
32. Kariya, Y., Ishida, K., Tsubota, Y., Nakashima, Y., Hirosaki, T., Ogawa, T., and Miyazaki, K. (2002) *J. Biochem. (Tokyo)* **132,** 607–612
33. Gehlsen, K. R., Sriramarao, P., Furcht, L. T., and Skubitz, A. P. (1992) *J. Cell Biol.* **117,** 449–459
34. Kikuchi, M., Hatano, N., Yokota, S., Shimozawa, N., Imanaka, T., and Taniguchi, H. (2004) *J. Biol. Chem.* **279,** 421–428
35. Kuster, B., Wheeler, S. F., Hunter, A. P., Dwek, R. A., and Harvey, D. J. (1997) *Anal. Biochem.* **250,** 82–101
36. Itoh, S., Kawasaki, N., Hashii, N., Harazono, A., Matsuishi, Y., Hayakawa, T., and Kawanishi, T. (2006) *J. Chromatogr. A* **1103,** 296–306
37. Gu, J., Sumida, Y., Sanzen, N., and Sekiguchi, K. (2001) *J. Biol. Chem.* **276,** 27090–27097
38. Isaji, T., Gu, J., Nishiuchi, R., Zhao, Y., Takahashi, M., Miyoshi, E., Honke, K., Sekiguchi, K., and Taniguchi, N. (2004) *J. Biol. Chem.* **279,** 19747–19754
39. Gu, J., and Taniguchi, N. (2004) *Glycoconj. J.* **21,** 9–15
40. Luo, B. H., Springer, T. A., and Takagi, J. (2003) *Proc. Natl. Acad. Sci. U. S. A.* **100,** 2403–2408
41. Fernandes, B., Sagman, U., Auger, M., Demetrio, M., and Dennis, J. W. (1991) *Cancer Res.* **51,** 718–723
42. Seelentag, W. K., Li, W. P., Schmitz, S. F., Metzger, U., Aeberhard, P., Heitz, P. U., and Roth, J. (1998) *Cancer Res.* **58,** 5559–5564
43. Handerson, T., and Pawelek, J. M. (2003) *Cancer Res.* **63,** 5363–5369
44. Le Marer, N., and Stehelin, D. (1995) *Glycobiology* **5,** 219–226
45. Bellis, S. L. (2004) *Biochim. Biophys. Acta* **1663,** 52–60
46. Chammas, R., Veiga, S. S., Travassos, L. R., and Brentani, R. R. (1993) *Proc. Natl. Acad. Sci. U. S. A.* **90,** 1795–1799
47. Yamamoto, H., Oviedo, A., Sweeley, C., Saito, T., and Moskal, J. R. (2001) *Cancer Res.* **61,** 6822–6829

Highlighted paper selected by Editor-in-chief

Quality Enhancement of the Non-immune Phage scFv Library to Isolate Effective Antibodies

Sunao IMAI,[a,b,#] Yohei MUKAI,[a,b,#] Kazuya NAGANO,[a,b] Hiroko SHIBATA,[a,b] Toshiki SUGITA,[a,b] Yasuhiro ABE,[a,b] Tetsuya NOMURA,[a,b] Yasuo TSUTSUMI,[a,b] Haruhiko KAMADA,[a] Shinsaku NAKAGAWA,[b] and Shin-ichi TSUNODA*,[a]

[a] *Laboratory of Pharmaceutical Proteomics, National Institute of Biomedical Innovation (NiBio); 7–6–8 Saito-Asagi, Ibaraki, Osaka 567–0085, Japan: and* [b] *Department of Biopharmaceutics, Graduate School of Pharmaceutical Sciences, Osaka University; 1–6 Yamadaoka, Suita, Osaka 565–0871, Japan.*

Received February 17, 2006; accepted March 23, 2006

The non-immune phage antibody library system is one of the most attractive technologies available to current therapeutic, diagnostic and basic scientific research. This system allows the rapid isolation of antibodies of interest that could subsequently be applied directly to drug delivery systems and antibody therapy. Previously, we reported the primer sets to encompass the antibody repertoire and thus improve library quality. However, a wide number of varying primer sets cause to decrease the amplification efficiency of antibody genes. In the present study, we re-generated the library primer sets newly and constructed an improved library from non-immune mice that was far superior in terms of variety and quality. This new library contained 2.4 billion independent clones. In addition, we optimized the selection step from this library to isolate high-affinity antibodies. The optimization of an affinity panning protocol by the incorporation of an automated Microfluidics instrument led to the successful isolation of three different monoclonal antibodies for human vascular endothelial growth factor receptor 2 (KDR). These antibodies were demonstrated to exhibit high specificity and were able to detect a mere 0.6 fmol of KDR by dot blot analysis. Previously reported antibodies for luciferase were also isolated successfully from this library. Our results clearly demonstrate the importance of the improved protocol for the library preparation of antibodies and the resulting isolation of antibodies for clinical and research applications.

Key words non-immune antibody library; phage display system; single-chain Fv; high-throughput screening; vascular endothelial growth factor receptor 2

Monoclonal antibodies are not only highly regarded as reagents for basic biochemical research but also for clinical diagnostic and therapeutic applications.[1—4] The production of a monoclonal antibody is laborious and time-consuming using established methodology involving the immunization of animals with large amounts of antigen, the isolation of B cells and the production of antibody-producing hybridomas. Therefore, the development of a rapid and easy method to produce monoclonal antibodies is highly desirable as an alternative to conventional hybridoma technology.[5,6]

Over recent years, phage display library technology has received a great deal of attention in terms of antibody production.[7—10] The phage display system is able to construct a large repertoire of protein or peptide libraries consisting of hundreds of millions of molecules. The phage antibody library which displays the single chain Fv fragment (scFv) of immunoglobulin is one of the most promising applications of the phage display system. Monoclonal antibodies against target antigens are obtained rapidly by the use of an affinity panning procedure *in vitro* which selects and amplifies the phage clones specific for the antigen required. There are two different types of phage antibody library system: the immune library made by using B cells isolated from patients or immunized animals as a gene source,[11] and the non-immune library made by using B cells isolated from healthy persons or non-immunized animals.[12,13] By using the non-immune library, antibodies for vast number of different kinds of antigens can be isolated without the need for *in vivo* immunization. However, several studies report that the common non-immune scFv libraries do not function effectively because of inefficiencies related to library preparation. The first problem associated with scFv library preparation is poor coverage of the PCR primer set used to amplify immunoglobulin genes. The second problem relates to the complicated procedure associated with the 3 fragment assembly which connects the VL and VH gene to a linker sequence. This assembly process is inefficient and often cause sequence frame shifts resulting in poor library quality.

In an attempt to overcome these problems, we previously attempted to construct a higher quality library by preparing an scFv library with improved PCR primer sets.[14] However, because the previous primer sets were constructed using mixed bases, the combinations of primer sets available to amplify the VL and VH fragments amounted to approximately two billion and six billion sets, respectively. Therefore, the ratio of one primer contained in primer sets was extremely low. In addition, because the amplification efficiency of PCR was extremely low, it was possible to incur bias in the amplification of antibody genes. Moreover, antibodies could not be isolated to some antigens using the previous library. In order to prepare a much better quality scFv gene library, it is necessary to re-design new primer sets for which the amplification efficiency of PCR is extremely high.

In the present study, we re-generated the original primer sets to remove any unnecessary primer variation whilst taking care to maintain sufficient diversity to encompass a wide variety of antibody genes. Using this new primer set, we were able to amplify antibody genes effectively and prepare a much better quality scFv gene library. Furthermore, we optimized the use of antibody selection methods with this new li-

* To whom correspondence should be addressed. e-mail: tsunoda@nibio.go.jp

# These authors contributed equally to the work.

brary and successfully isolated several high affinity clones specific for a tumor endothelial marker, KDR.[15,16]

MATERIALS AND METHODS

Construction of scFv Genes Total RNA was extracted from spleen cells and femoral bone marrow cells prepared from non-immunized 6-week-old male C57BL/6, Balb/c, and C3H mice. The mRNA was purified using a mRNA Purification Kit (Amersham Biosciences, Piscataway, NJ, U.S.A.) and first-strand cDNA was synthesized with the SuperScript™ III First-Strand Synthesis System for RT-PCR (Invitrogen, Carlsbad, CA, U.S.A.). From each cDNA, immunoglobulin heavy-chain and light-chain genes were separately amplified and recombined by three subsequent PCR reactions as follows. In the first-step PCR, variable regions of the heavy and light chain genes (VH and VL) were amplified. The light chain 5′ primers were modified to include an *Nco* I site, and heavy chain 3′ primers to include a *Not* I site. Light chain 3′ primers were designed to assemble with heavy chain 5′ primers (Fig. 1). Light and heavy chain variable region genes were amplified by PCR reaction containing 1 μl of RT PCR products (cDNA) and 2 pmol of each primer set. The samples were cycled 35 times at 96 °C for 60 s, 50 °C for 60 s, and 68 °C for 60 s. The PCR products were then purified using a QIAquick PCR Purification Kit (QIAgen, Valencia, CA, U.S.A.). In the second PCR, equal amounts of the previously amplified VL and VH DNA were mixed and cycled 20 times at 96 °C for 60 s, 63 °C for 60 s, and 68 °C for 60 s without primers. The resulting PCR products, the scFv gene library, were then purified using a QIAquick PCR Purification Kit. In the third-step, the additional sequences were extended from *Nco* I and *Not* I sites upstream of the scFv gene library by overlap PCR using primer Y15 (5′-GCCAAGCTTTGGAGCCTTTTTTTTGGAGATTTTCAACGTGAAAAAATTATTATTCGCAATTCCTTTAGTTGTTCCTTTCTATGCGGCCCAGCCGGCCATGGCC-3′) and primer Y16 (5′-TTAGTAAATGAATTTTCTGTATGAGGTTTTGCTAAACAACTTTCAACAGTCTATGCGGCACGCGGTTCCACGGATCCGGATACGGCACCGGCGCACCTGCGGCCGC-3′) by cycling 35 times at 96 °C for 60 s, 65 °C for 60 s, and 68 °C for 60 s.

Construction of Non-immune Mouse scFv Phage Libraries and DNA Sequencing The PCR amplified scFv genes and pCANTAB5E phagemid vector were digested with *Nco* I and *Not* I. The resultant scFv fragments were inserted into the pCANTAB5E vector to generate a scFv-gene III fusion library, using T4 ligase (Roche Diagnostics, Indianapolis, IN, U.S.A.) at 16 °C for 16 h. The ligated product, *E. coli* TG1 was transformed by electroporation and grown at 37 °C on culture plates containing 2YT medium supplemented with 100 μg/ml ampicillin and 2% glucose (2YTAG medium). Twelve clones were selected at random and insert plasmid DNA was sequenced and analyzed.

Phage Purification A scFv phage library containing 2.4×10^9 clones was used for the affinity selection. Glycerol stocks of the scFv library were grown in the log phase, rescued with M13KO7 helper phage (Invitrogen) and then amplified at 37 °C for 6 h in 2YT medium supplemented with 100 μg/ml ampicillin and 50 μg/ml kanamycin. The phage was subsequently precipitated with PEG–NaCl (4% PEG, 0.5 M NaCl) and then resuspended in NTE buffer (100 mM NaCl, 10 mM Tris, and 1 mM EDTA).

Affinity Panning Affinity panning was performed by using the BIAcore 3000 system (BIAcore, Uppsala, Sweden). The sensor chip CM3 (BIAcore) was modified with 5 μg of antigen (KDR-Fc chimera; R&D systems Inc., Minneapolis, MN, U.S.A.) or luciferase (Promega Co., Madison, WI, U.S.A.). The scFv phage library was then incubated with 50% HBS-EP buffer (BIAcore) and loaded onto the antigen-immobilized sensor chip. After the binding step, the sensor chip was rinsed with HBS-EPT (HBS-EP containing 0.05% Tween 20). Bound phage was then eluted with Glycine–HCl buffer (pH 2) and Glycine–NaOH buffer (pH 11). These processes were regulated by BIAcore Control Software. The eluted phage was then incubated in log phase TG1 cells and glycerol stocks prepared for further repeat panning cycles. Phage titer was measured by counting the number of infected colony cells on Petrifilm (3M Co., St. Paul, MN, U.S.A.).

Phage ELISA Following the panning process, individual TG1 clones were picked, grown at 37 °C in 96-well plates and then rescued *via* M13KO7 helper phage infection. The amplified phage preparation was then blocked with 2% Block Ace (Dainippon Sumitomo Pharma Co., Osaka, Japan) at 4 °C for 1 h and then added to an immunoassay plate

VL Forward	5′-cctttctatgcggcccagccgg**CCATGG**cc- -GAYATTGTWCTCWCCCARTC -3′ -GAYRTTKTGATGACCCAVAC -3′ -GAYATTSTGMTSACYCAGTC -3′ -GAYATYCAGATGACACAGAC -3′ -GAYATTGTGMTMACTCAGTC -3′ -GAYATTGTGATGACACAACC -3′ -GAYATTGTGHTRWCACAGTC -3′ -GAYATCCAGCTGACTCAGCC -3′ -GAYATTGTRATGACMCAGTC -3′ -GAYATTGTGATGACBCAGKC -3′ -GAYATTMAGATRAMCCAGTC -3′ -GAYATTGTGATAACYCAGGA -3′ -GAYATTCAGATGAYDCAGTC -3′ -GAYATTGTGATGACCCAGWT -3′ -GAYATTTTGCTGACTCAGTC -3′ -GAYGTGSTGMTSACYCAGTC -3′ -GAYATTGTTCTCAWCCAGTC -3′ -GAYGCTGTTGTACTCAGGAATC -3′ -GAYATTGWGCTSACCCAATC -3′ -GAYATTGTDHTVWCHCAGTC -3′ -GAYATTSTRATGACCCARTC -3′
VL Reverse	5′-accagagccgccgccgccgctaccaccaccacc- -CCGTTTGATTTCCARCTTKG -3′ -CCGTTYWATTTCCAACTTWG -3′ -CCGTTTTATTTCCAGCTTGG -3′ -CCCTAGGACAGTCAGTTTGG -3′ -CCGTTTSAGCTCCAGCTTGG -3′
VH Forward	5′-agcggcggcggcggctctggtggtggtggatcc- -GAKGTRMAGCTTCAGGAGYC -3′ -SAGGTGCAGSKGGTGGAGTC -3′ -GAGGTNCAGCTBCAGCAGTC -3′ -GAKGTGCAMCTGGTGGAGTC -3′ -CAGGTGCAGCTGAAGSASTC -3′ -GAAGTGCAVCTGGTGGAGTC -3′ -CAGSTBCAGCTGCAGCAGTC -3′ -GAGGTGAAGCTGATGGARTC -3′ -GAGGTYCAGCTYCAGCAGTC -3′ -GAGGTGCARCTTGTTGAGTC -3′ -GARGTCCARCTGCAACARTC -3′ -GARGTRAAGCTTCTCGAGTC -3′ -CAGGTYCAGCTBCAGCARTC -3′ -GAAGTGAARSTTGAGGAGTC -3′ -CAGGTYCARCTKCAGCAGTC -3′ -GAAGTGATGCTGGTGGAGTC -3′ -CAGGTCCACGTGAAGCAGTC -3′ -CAGGTTACTCTRAAAGWGTSTG -3′ -GAGGTGAASSTGGTGGARTC -3′ -CAGGTCCAAYTVCAGCARCC -3′ -GAVGTGAWGYTGGTGGAGTC -3′ -GATGTGAACTTGGAAGTGTC -3′ -GAGGTGAAGGTCATCGAGTC -3′
VH Reverse	5′-cggcaccggcgcacct**GCGGCCGC**- -YGAGGAAACGGTGACCGTGGT -3′ -YGAGGAAGACTGTAGAGTGGT -3′ -YGAGGAGACTGTGAGAGTGGT -3′ -YGCGGAGACASTGACCAGAGT -3′ -YGAGGAGACGGTGACTGAGRT -3′ -YGCAGAGACASTGACCAGAGT -3′

S=G/C, R=G/A, K=G/T, M=A/C, Y=C/T, W=A/T, H=A/C/T, B=C/G/T, V=A/C/G, D=A/G/T, N=A/T/G/C

Fig. 1. Primers for PCR Amplification of VL and VH

New primer sets were designed that allowed immunoglobulin genes to be amplified as efficiently as possible by referring previous reports and the Kabat Database. Linker sequences were added downstream of the VL gene primers and upstream of the VH gene primers so that the amplified VL and VH genes could be easily connected.

coated with the antigens. Plates were then incubated for 2—3 h, with agitation at 250 rpm, and were then washed three times with phosphate buffered saline/0.1% Tween 20 (PBST), and finally incubated with HRP-conjugated anti-M13 monoclonal antibody (Amersham Bioscience). Plates were then washed once more with PBST and then TMB peroxidase substrate (MOSS, INC.) was added. Absorbance was then measured at 450 nm and 655 nm as a reference.

Dot Blot Analysis Antigens were immobilized on nitrocellulose membranes using the Bio-Dot Microfiltration Apparatus (Bio-Rad Laboratories, Hercules, CA, U.S.A.). The membrane was incubated with blocking solution (10% skimmed milk, 25% glycerol) for 2 h and then washed twice with TBST (Tris buffered saline containing 0.1% Tween 20). The phage preparation was pre-incubated with 90% blocking solution at 4 °C for 1 h and then applied to each well. After 2—3 h incubation, the apparatus was washed five times with TBST and then incubated with HRP-conjugated anti-M13 monoclonal antibody. After three further washes with TBST and TBS, the membrane was treated with ECL-Plus reagent (Amersham Bioscience) and detected by use of a CCD image analyzer (LAS-3000, Fuji Photo Film Co. Ltd., Kanagawa, Japan).

RESULT AND DISCUSSION

In this study, we aimed to isolate a scFv monoclonal antibody from a non-immune antibody phage display library constructed using our improved PCR primer set. We specifically designed the primer sets to produce a non-immune antibody library that was superior in variety and accuracy than the past libraries (Fig. 1). To begin with, we re-designed primers which allowed immunoglobulin genes to be amplified as efficiently as possible by excluding an unnecessary mixture of bases from the previous primer sets. The combinations of primers to amplify the VL and VH genes were approximately four thousand and three thousand sets, respectively. Furthermore, the combination of primer sets to construct a scFv gene was more than ten million. The diversity of this primer set increased by approximately 10000-fold in comparison with that of the past reports. In addition, by using these primer sets randomly, we confirmed that the PCR products were gotten from all reactions (data not shown). In addition, in accordance with our previous report, linker sequences were added downstream of the VL gene primers and upstream of the VH gene primers such that the amplified VL and VH genes were easily connected, thereby reducing the possibility of frame shift in the sequence. Using the modified primer sets, the non-immune murine scFv phage library was prepared by the method described in our previous report.[14]

The titer of the resultant scFv phage library was 2.4×10^9 cfu. The repertoire of this library was as diverse as that of the library previously reported. DNA sequence analysis of twelve clones picked randomly from the library demonstrated no evidence of frame shift in the scFv genes (Fig. 2). Because the diversity of the CDR3 domain that is important for antigen binding is estimated to be in the region of twenty million, we suggest that our new scFv library has almost equal potential as the murine or human immune system.[18,19] Additionally, because the pIII protein of phage is generally toxic against *E. coli*, it was likely that contamination of the plasmid coding for the frame-shifted scFv gene promotes the production of the wild type phage that does not display antibody (data not shown). This means that we could not isolate

VL

	FR1	CDR1	FR2	CDR2	FR3	CDR3	FR4	Linker
1	DIVMTQSHKFMSTSVGDRVSITC	KASQDVSTAVA	WYQQKPGQSPKLLIY	SASYRYS	GVPDRFTGSGSGTDFTLTISNVQAEDLAVYYC	QQYNSYPYT	FGGGTKLEIKR	GGGGSGGGGSGGGGS
2	-------PSS-YA-L-E--T---	-----INSYLS	-F-----K---T---	R-NRLVD	---S--S-----Q-YS----SLEY--MGI---	LLSTVSS--	----------	----------
3	------TPLTL-VTI-QPA--S-	-S--SLLDSDGKTYLN	-LL-R------R---	LV-KLD-	----------K--R-E----G----	W-GTHF-R-	----------	----------
4	--Q---AAPSVPVTP-ES---S-	RS-KSLLHSDGNTYLY	-FL-R-----Q----	RM-NLA-	------S------A---R--R-E---VG----	M-HLE--L-	--A-------	----------
5	-------Q----------V--	----N-G-N--	---------A---	-------	----------S----E-F-	---------	----------	----------
6	--LL----------	----------	----------	W--T-HT	----------Y-----S------L---	--HY-T-L-	--A-----LE-	----------
7	--E----Q----------V--	----N-G-N--	---------A---	-------	----------S----E-F-	-------L-	--------L--	----------
8	N------Q----------V--	----N-G-N--	---------A---	YT-RLH-	----------S----E-F-	-------L-	----------	----------
9	-------PAI-A--P-EK-TM--	S-SS-SYMH	-----S-T---RW--	DT-KLA-	---A--S------SYS----R-E---A-T---	--WS-N-P-	--A-------	----------
10	----------	----------	----------	W--TRHT	----------S----E-F-	---------	--------L--	----------
11	---LN----------	----------	----------	------T	----------F---S----------	--HY-T---	--------L--	----------
12	----------	------G----	----------	W--T-HT	----------Y-----S------L---	--HY-T---	----------	----------

VH

	FR1	CDR1	FR2	CDR2	FR3	CDR3	FR4
1	EVQLVESGGGLVKPGGSLKLSCAASGFTFS	SYGMS	WVRQTPEKGLEWVA	YISSGGSTTYYPDSVKG	RFTISRDNAKNTLYLQMSSLKSEDTAMYYCAR	GGGVFYDY	WGQGTTLTVSS
2	Q---QQ-AE------A-V-I--K---YA--	--W-N	--K-R-G-----IG	Q-YP-DGD-N-NGKF--	KA-LTA-KSSS-A-MQL---T---S-V-F--G	GTYYFDY	----------
3	D-H----------R----------	--T--	--------R-----	------GN---------	---------R----------R----------	GHY	----------
4	--HW----------	D---H	----A---------	-----S--I--A-T---	----------F---T--R----------	LTTVVDY	----------
5	--K---------Q----------	-----	------D-R--L--	T-N-N-GS---------	----------	DGNLYLLAY	-----LV---
6	--N----------	--T--	--------R-----	------GN---------	---------R----------R----------	RGNYYDYDGYFDV	--A---V----
7	----------Q----------	D---H	----A---------	-----S--I--A-T---	--------P----F----------T-	GTNWDYFDY	----------
8	--K-----E----------	--A--	--------R-----	------DYI--A-T---	---------R----------T-	EERYYPDY	----------
9	--M----E----Q--S--M----T------	D-Y-A	----------	N-NYD--S---L--L-S	--I---------I----------T-----	DLYYFDY	----------
10	---R----------	--A--	--------R-----	T--D---Y---------	----------N----------K	HGGSSYGFAY	-----LV---
11	--K----E----Q--S--M----T------	D-Y-A	----V---------	N-NYD--S---L--L-S	--I---------I----------T---T-	RGGTVCFDY	----------
12	Q---QQ-AE------A-V-I--K---YA--	SSWM-N	--K-R-G-----IG	R-YP-DGD-N-NGKF--	KA-LTA-KSSS-A-MQL---T---S-V-F---	DDD	----------

Fig. 2. Predicted Amino Acid Sequences of Non-immune Library

Amino acid sequences of 12 clones which were randomly picked from the library and analyzed by DNA sequence.

antibodies by pannig because the wild type phage is amplified faster than the antibody displaying phage. However, we strongly believe that this library was of high quality because all randomly-picked clones maintained the scFv sequence.

To obtain an antibody for a target antigen by using the phage display system, it is important to effectively increase the phage clones interact with the target antigen by repeated affinity panning. Although an immunoplate or immunotube is commonly used for the affinity panning,[20,21] it is commonly known that these techniques are inefficient in terms of antibody enrichment, are difficult to automate and exhibit difficulties in controlling the precise settings for panning conditions. Therefore, our present study utilized an automated microfludics system with a surface plasmon resonance analyzer (BIAcore 3000, BIAcore International AB, Uppsala, Sweden) to ensure that the panning procedure was both easy and optimized.

Generally, either acidic or basic solutions are required for the elution step during panning.[12,22] In our study, both acidic (pH 2) and basic (pH 11) buffers, containing a surfactant, were used for the elution step to completely dissociate the entrapped antibodies at high affinity. To evaluate the usefulness of the library, affinity panning against the human KDR, as a model antigen, was performed (Fig. 3). The experiment involving two rinse procedures exhibited an increase of approximately 100 fold in the ratio of phage titer after the fifth panning, while the experiment involving ten rinses exhibited a 1000-fold increase (Fig. 3A). Additionally, phage ELISA

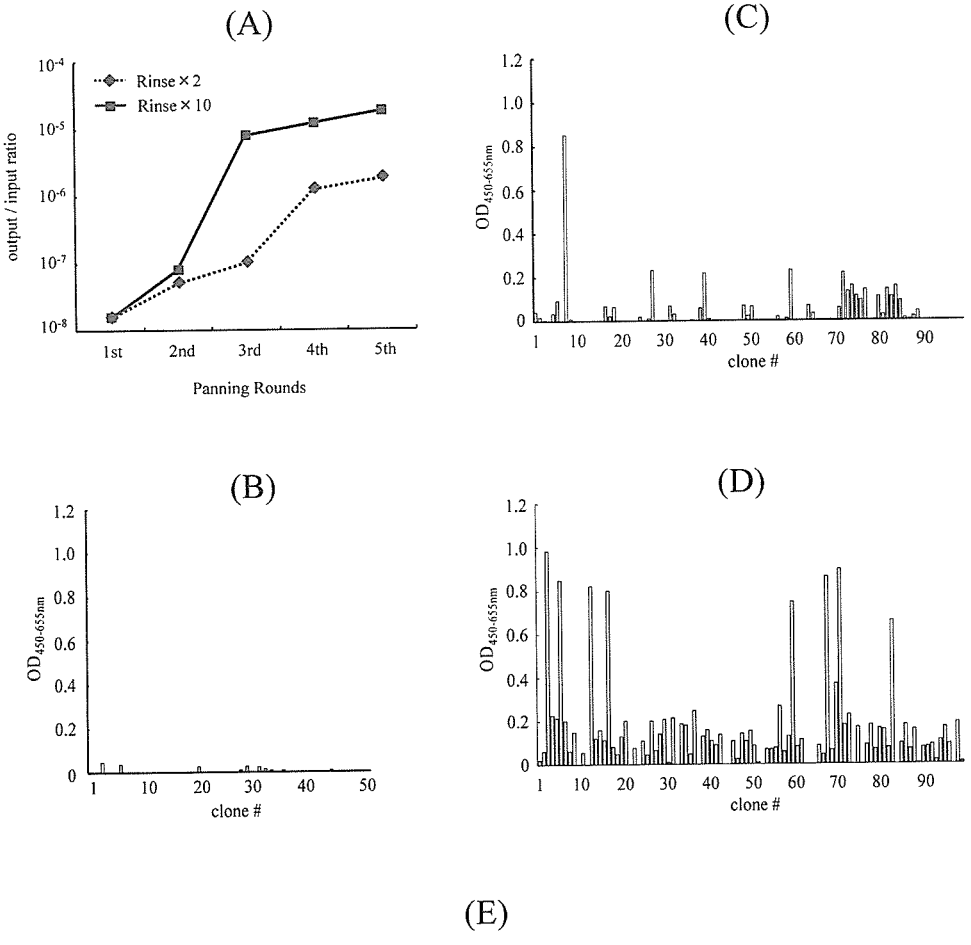

(E)

VL

	FR1	CDR1	FR2	CDR2	FR3	CDR3	FR4	Linker
anti-KDR-1	DIVMTQSPATLSVTPGDRVSLSC	RASQNISAYLH	WYQQKSHESPRLLIK	YASQSIS	GIPSRFSGSGSGS-FTLSINSVEPEDVGVYYC	QNGHSFPYT	FGGGTKLEIKR	GGGGSGGGGSGGGGS
anti-KDR-2	-------QKFM-TSV-----VT-	K----VGTNVA	-----PGQ--KA--Y	S--YRY-	-V-D--T-----TD---T-SN-QS--LAE-F-	-QYN-Y-W-	--------L--	---------------
anti-KDR-3	-------HKFM-TSV-----VT-	K----VGTNVA	-----PGQ--KA--Y	S--YRY-	-V-D--T-----TD---T-SN-QS--LAE-F-	-QYN-Y-LL-	--A-----I--	---------------

VH

	FR1	CDR1	FR2	CDR2	FR3	CDR3	FR4
anti-KDR-1	EVKLVQSGAELVRPGTSVKLSCKASGYTFT	SYWMH	WVKQRPGQGLEWIG	AIYPGNSDTSYNQKFKGKAKLTAVTSASTAYMELSSLTNEDSAVYYCTR	EWDYYAMDY	WGQGTSVTVSS	
anti-KDR-2	Q-QV-E--GG--K--G-L----A---F--S	--A-S	--R-T-EKR---VA	T-SS-G-Y-Y-PDSV--RFTISRDNAKN-L-LQM---RS--T-M---A-	QRRDGSIWYFDV	--A--T-----	
anti-KDR-3	E-QL-E--GG--Q--G-L----A---F--S	--G-S	--R-T-DKR---VA	T-SS-G-Y-Y-PDSV--RFTISRDNAKN-L-LQM---KS--T-M---A-	HYYGSSYYFDY	-----TL----	

Fig. 3. Enrichment and Cloning of Antibodies to Human KDR from Non-immune scFv Phage Library by Affinity Panning

Enrichment of the desired clones was performed by affinity panning on the immobilized human KDR using the BIAcore 3000 system. (A) The ratio of phage titer at each panning round was plotted. The ratio was calculated as follows: (titer of the output phage)/(titer of the input phage). The closed line represents the data from the procedure involving ten rinses and the dashed line represents the data involving two rinses (B). After the fifth panning on human KDR, the binding properties of the selected phage clones were analyzed by ELISA. The data represent the results of measurement of clones before panning (B), after fifth panning involving two rinses (C) and after fifth panning with ten rinses (D). (E) Amino acid sequences of 8 clones high affinity clones for human KDR analyzed by DNA sequence.

analysis of 250 randomly picked clones showed that the number of positive clones binding to the KDR in the experiment involving ten rinses was higher than that involving two rinses (Figs. 3B—D). These results demonstrated that an optimized panning procedure with ten rinses effectively enriched the antibody clones specific for the target antigen. DNA sequence analysis of the eight clones of high affinity for human KDR demonstrated that these clones consisted of three different arrangements of antibodies (Fig. 3E). And then, we also confirmed that soluble formed scFvs of them could bind to KDR (data not shown). ELISA also demonstrated that these anti-KDR antibodies reacted not only with human KDR but also with murine KDR at similar affinity (Fig. 4). Because of natural tolerance, it is generally difficult to obtain an antibody to not only an antigen which has high homology but also an allogeneic antigen of the immunized animal. However, in our experiment, anti-KDR scFvs isolated from a non-immune mouse antibody library were able to bind murine KDR (allogeneic antigen). Therefore, it is suggested that these antibodies are of great importance to both mouse models and human research. This is because the non-immune scfv phage library, constructed by connecting VL and VH genes *in vitro*, included a nonexistent repertory naturally. This result shows that our non-immune scFv phage library is a useful technological resource for producing antibodies to autoantigens

We then investigated the binding specificity of the three anti-KDR scFv antibodies by dot blot assay. These antibodies could bind native and denatured KDR, but not other antigens, tumor necrosis factor receptor 2 (TNFR2), luciferase, bovine serum albumin (BSA), importin-α, and importin-β (Fig. 5). The fact that these scFvs did not react to the TNFR2-Fc chimera indicates that these reacted not with the Fc domain but rather the KDR domain. It was also revealed that the sensitivity of dot blot analysis using the three scFvs as primary antibodies was as high as the level of detection of 100 pg (0.6 fmol) of immobilized antigen by anti-KDR-1 and anti-KDR-3 and 10 ng (60 fmol) by anti-KDR-2 (Fig. 6). The detection limit of general antibodies of the IgG type is approximately 1 ng (data not shown). In contrast, anti-KDR-1 and anti-KDR-3 antibodies could detect 100 pg of KDR. The data therefore suggests that the affinity of anti-KDR scFv antibodies is better than antibodies of the IgG type. This shows that the anti-KDR antibodies obtained from our library were of high quality and could recognize very small amounts of antigen.

To examine the usefulness of the library, we tried to isolate an antibody to a previously reported antigen, luciferase (Fig. 7). As panning to the luciferase was repeated, the output/input ratio was gradually elevated and the enrichment of the library reached approximately 5000-fold after the fifth pan-

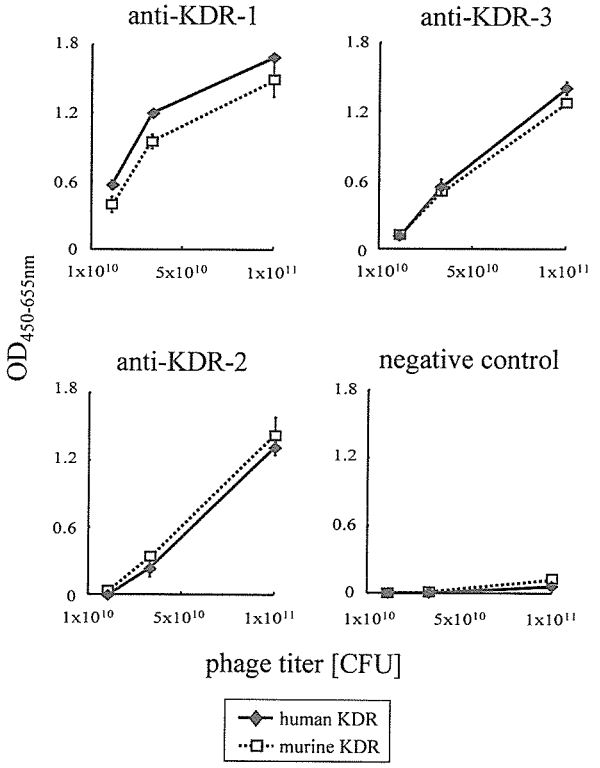

Fig. 4. Binding Properties of the Isolated Anti-KDR scFv Antibodies against Human or Murine KDR

The binding properties to human KDR (◆) and murine KDR (□) of anti-KDR scFvs displayed on the phage surface were measured by ELISA as described in the Materials and Methods. Three phage clones, anti-KDR-1, anti-KDR-2, and anti-KDR-3 were analyzed. A clone displaying scFv to luciferase was used as a negative control.

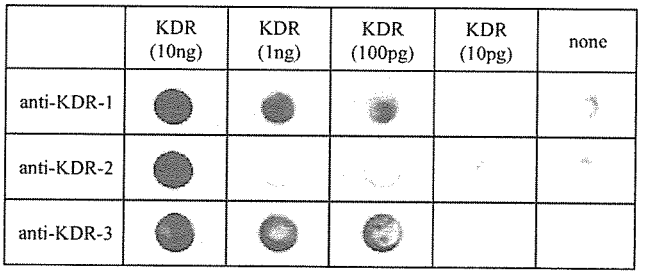

Fig. 6. Sensitivity of Antigen Detection by Anti-KDR scFvs

Anti-KDR scFv phages were reacted with KDR-Fc chimera (10 ng, 1ng, 100 pg and 10 pg in each spot) immobilized on a nitrocellulose membrane using a dot blot manifold.

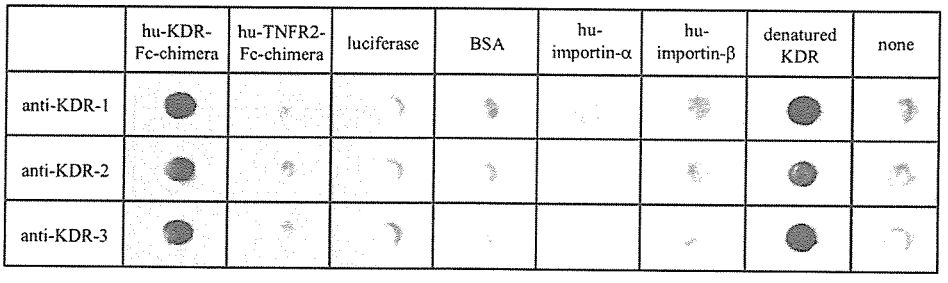

Fig. 5. Binding Specificity of Anti-KDR scFv Antibodies

Binding specificity of anti-KDR scFvs was examined by dot blot analysis. Native hu-KDR-Fc-chimera, hu-TNFR2-Fc-chimera, luciferase, BSA, hu-importin-α, hu-importin-β and denatured hu-KDR (100 ng each) were dot blotted onto a nitrocellulose membrane and then the purified anti-KDR scFvs phage was reacted in the wells.

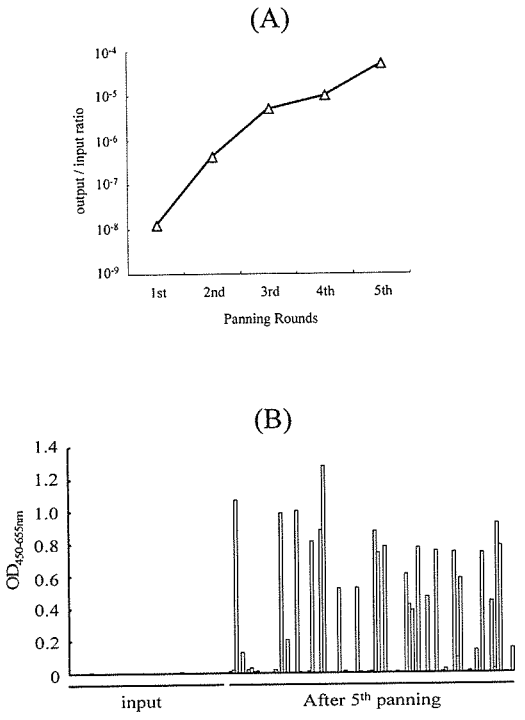

Fig. 7. Enrichment and Cloning of scFv Antibodies to Luciferase

Anti-luciferase scFv phages were selected from the non-immune phage library. Five rounds of affinity panning to the luciferase were performed using the BIAcore 3000 system. The ratio of the titer of output phage/input phage at each panning round was plotted (A). After fifth panning, the scFv phage clones of affinity with luciferase were analyzed by ELISA (B).

ning (Fig. 7A). A total of 150 phage clones were randomly picked and their binding to luciferase tested by ELISA (Fig. 7B). The number of positive clones was increased by affinity panning to luciferase and a high number of clones were successfully isolated. Because the variety of previous primer sets was very excessive, the amplification efficiency of PCR was extremely low. On the other hand, we confirmed that all combinations of these primer sets could amplify effectively. Moreover, antibodies to some antigens could not be isolated from the previous library. Using the present library, however, antibodies to all ten kinds of antigens tested were successfully isolated (data not shown). In addition, anti-KDR scFvs isolated from the present library were far superior in terms of antigen specificity and sensitivity and were able to bind an allogeneic antigen. Collectively, these results suggest that the present library was far superior to the previous one.

Over recent years it has become highly expected that antibodies should be able to be applied not only as a biochemical reagent for basic research but also as diagnostic tools and antibody-based medicine.[23—27] It is therefore vital to be able to obtain the desired antibody for various antigens rapidly. Because the non-immune scFv antibody phage library reported here can isolate antibodies for various antigens *in vitro*, we suggest that this resource will prove highly beneficial for future research and clinical applications.

Acknowledgments This study was supported in part by Grants-in-Aid for Scientific Research (No. 17689008, 17016084, 17790135, 18015055, 18659047) from the Ministry of Education, Culture, Sports, Science and Technology of Japan, a Health and Labor Sciences Research Grant from the Ministry of Health, Labor and Welfare of Japan, Industrial Technology Research Grant Program (No. 03A47016a) from New Energy and Industrial Technology Development Organization (NEDO), and JSPS Research Fellowships for Young Scientists (No. 08476, 08841, 09131) from the Japan Society for the Promotion of Science.

REFERENCES

1) Baert F., Noman M., Vermeire S., Van Assche G., D'Haens G., Carbonez A., Rutgeerts P., *N. Engl. J. Med.*, **348**, 601—608 (2003).
2) Plosker G. L., Figgitt D. P., *Drugs*, **63**, 803—843 (2003).
3) Hurwitz H., Fehrenbacher L., Novotny W., Cartwright T., Hainsworth J., Heim W., Berlin J., Baron A., Griffing S., Holmgren E., Ferrara N., Fyfe G., Rogers B., Ross R., Kabbinavar F., *N. Engl. J. Med.*, **350**, 2335—2342 (2004).
4) A security-related information magazine of France, (no authors), *Prescrire Int.*, **14**, 215—217 (2005).
5) Kohler G., Hengartner H., Shulman M. J., *Eur. J. Immunol.*, **8**, 82—88 (1978).
6) Daigo K., Sugita S., Mochizuki Y., Iwanari H., Hiraishi K., Miyano K., Kodama T., Hamakubo T., *Anal. Biochem.*, **351**, 219—228 (2006).
7) Smith G. P., *Science*, **228**, 1315—1317 (1985).
8) McCafferty J., Griffiths A. D., Winter G., Chiswell D. J., *Nature* (London), **348**, 552—554 (1990).
9) Clackson T., Hoogenboom H. R., Griffiths A. D., Winter G., *Nature* (London), **352**, 624—628 (1991).
10) Pini A., Bracci L., *Curr. Protein Pept. Sci.*, **1**, 155—169 (2000).
11) Rojas G., Almagro J. C., Acevedo B., Gavilondo J. V., *J. Biotechnol.*, **94**, 287—298 (2002).
12) Vaughan T. J., Williams A. J., Pritchard K., Osbourn J. K., Pope A. R., Earnshaw J. C., McCafferty J., Hodits R. A., Wilton J., Johnson K. S., *Nat. Biotechnol.*, **14**, 309—314 (1996).
13) Goletz S., Christensen P. A., Kristensen P., Blohm D., Tomlinson I., Winter G., Karsten U., *J. Mol. Biol.*, **315**, 1087—1097 (2002).
14) Okamoto T., Mukai Y., Yoshioka Y., Shibata H., Kawamura M., Yamamoto Y., Nakagawa S., Kamada H., Hayakawa T., Mayumi T., Tsutsumi Y., *Biochem. Biophys. Res. Commun.*, **323**, 583—591 (2004).
15) Vitaliti A., Wittmer M., Steiner R., Wyder L., Neri D., Klemenz R., *Cancer Res.*, **60**, 4311—4314 (2000).
16) Izumi Y., di Tomaso E., Hooper A., Huang P., Huber J., Hicklin D. J., Fukumura D., Jain R. K., Suit H. D., *Cancer Res.*, **63**, 747—751 (2003).
17) The Kabat Database of Sequences of Protein of immunological Interest. Available from: ⟨http://www.kabatdatabase.com⟩
18) Tonnelle C., Cuisinier A. M., Gauthier L., Guelpa-Fonlupt V., Milili M., Schiff C., Fougereau M., *Ann. N.Y. Acad. Sci.*, **764**, 231—241 (1995).
19) Xu J. L., Davis M. M., *Immunity*, **13**, 37—45 (2000).
20) Sheets M. D., Amersdorfer P., Finnern R., Sargent P., Lindquist E., Schier R., Hemingsen G., Wong C., Gerhart J. C., Marks J. D., *Proc. Natl. Acad. Sci. U.S.A.*, **95**, 6157—6162 (1998).
21) Fraile S., Roncal F., Fernandez L. A., de Lorenzo V., *J. Bacteriol.*, **183**, 5571—5579 (2001).
22) Coomber D. W., *Methods Mol. Biol.*, **178**, 133—145 (2002).
23) Ross J. S., Gray K., Gray G. S., Worland P. J., Rolfe M., *Am. J. Clin. Pathol.*, **119**, 472—485 (2003).
24) Ross J., Gray K., Schenkein D., Greene B., Gray G. S., Shulok J., Worland P. J., Celniker A., Rolfe M., *Expert. Rev. Anticancer Ther.*, **3**, 107—121 (2003).
25) Valle R. P., Jendoubi M., *Curr. Opin. Drug Discov. Devel.*, **6**, 197—203 (2003).
26) Russeva M. G., Adams G. P., *Expert. Opin. Biol. Ther.*, **4**, 217—231 (2004).
27) Adams G. P., Weiner L. M., *Nat. Biotechnol.*, **23**, 1147—1157 (2005).

Creation of Novel Protein Transduction Domain (PTD) Mutants by a Phage Display-Based High-Throughput Screening System

Yohei MUKAI,[a,b,#] Toshiki SUGITA,[a,b,#] Tomoko YAMATO,[a,b,#] Natsue YAMANADA,[a,b] Hiroko SHIBATA,[a,b] Sunao IMAI,[a,b] Yasuhiro ABE,[a,b] Kazuya NAGANO,[a,b] Tetsuya NOMURA,[a,b] Yasuo TSUTSUMI,[a,b] Haruhiko KAMADA,[a] Shinsaku NAKAGAWA,[b] and Shin-ichi TSUNODA*,[a]

[a] *Laboratory of Pharmaceutical Proteomics, National Institute of Biomedical Innovation; 7–6–8 Saito-Asagi, Ibaraki, Osaka 567–0085, Japan: and* [b] *Department of Biopharmaceutics, Graduate School of Pharmaceutical Sciences, Osaka University; 1–6 Yamadaoka, Suita, Osaka 565–0871, Japan.* Received March 23, 2006; accepted May 11, 2006

Significant research effort is currently focused on Protein Transduction Domains (PTDs) as potential intracellular drug delivery carriers. However, the application of this technology is limited because the transduction efficiencies are often insufficient for therapeutic purposes, even using HIV-1 Tat peptide. Here we describe a high-throughput screening method based on a phage display system for isolating novel PTDs with improved cell penetration activity. The screening method involves using protein synthesis inhibitory factor (PSIF) as cargo of PTD. Using this method, several Tat-PTD mutants of superior cell-penetrating activity were isolated. Interestingly, the amino acid sequence of the PTD mutants contained some characteristic residues, such as proline. Thus, our screening method may prove useful in determining the relationship between protein transduction and amino acid sequence.

Key words phage display system; protein transduction domain; high-throughput screening; HIV-1 Tat; intracellular drug delivery

Recent advances in proteomics have allowed a number of refractory diseases, such as cancer and neurodegenerative disorders, to be studied at the molecular level. The main causative factor of such disease states is often associated with intracellular organelles or particular subcellular proteins. Thus, the intracellular organelles, proteins or genes might constitute the therapeutic target. Recently, it was discovered that certain peptides, referred to as protein transduction domains (PTDs), can penetrate cells accompanied by a large molecular cargo. Considerable research effort is currently focused on utilizing PTDs as peptide-based carriers for intracellular drug delivery.[1—3]

Tat peptide, derived from the HIV-1, and Antennapedia peptide, derived from Drosophila Antennapedia homeotic transcription factor, are well known PTDs that have been tested as drug delivery carriers for various disease models.[4—9] PTDs can even deliver bulky molecular cargos (>100 kDa) into a wide variety of cell types.[10—13] However, to use PTDs as effective intracellular drug delivery carriers with clinical applications, it is necessary to create novel PTDs with greater protein-transduction potency than exists naturally.

An attempt to create a novel PTD by modification of the peptide structure has already been reported.[14,15] However, because it is difficult to predict the transduction activity of the peptide based on structural information alone, novel peptides must be generated by introducing amino acid substitutions and then the effects determined by trial and error. Recently, we have successfully generated a technology for creating novel muteins (mutant proteins) that have non-native functions using a phage display system.[16] This prompted us to apply phage display technology to screen for novel PTDs.

The phage display system is a protein selection methodology in which a library of mutant proteins or peptides can be screened and the desired molecules easily identified by linking DNA information (genotype) with phenotype (protein expression).[16—20] By applying this methodology, novel PTDs can be selected such as those transduced into the cell by a different mechanism or those with tissue/cell specificity. In general, the phage display system is used to isolate antibody and peptide ligands using an affinity selection step to target the desired molecules. However, for the discovery of PTDs it is necessary to construct a screening method to select clones that are transduced into the cell rather than simply selecting those that bind to the cell surface. We designed a high-throughput screening method to isolate effective PTDs by fusing PTD with Protein Synthesis Inhibitory Factor (PSIF).[21] Here, we used our methodology to identify novel Tat mutants with greater transduction potency than wild-type Tat PTD.

MATERIALS AND METHODS

Library Construction A gene library of Tat mutant peptides was constructed by randomization of codons (except arginine codons) of Tat [47—57] using PCR primers containing NNS sequences (N; A/T/G/C, S; G/C). Two primer sequences were used in this PCR. Forward primer, Y-oligo22 3′ ex (5′-TCA CAC AGG AAA CAG CTA TGA CCA TGA TTA CGC CAA GCT TTG GAG CC-3′) contained a *Hind*III site and annealed on pCANTAB phagemid vector. Reverse primer, Tat[47—57] R (5′-TC ATC CTT GTA GTC TGC GGC CGC ACG ACG ACG SNN ACG ACG SNN SNN ACG SNN SNN GGC CAT GGC CGG CTG GGC CGC ATA GA AAG-3′) contained five NNS codons and a *Not*I site. After amplification of the Tat[47—57] mutant gene, the PCR fragments were digested with *Hind*III and *Not*I and cloned into the pCANTAB phagemid vector (Invitrogen Corp., Carlsbad, CA, U.S.A.). *E. coli* TG1 cells (Stratagene, La Jolla, CA, U.S.A.) were transformed with the phagemid by electroporation and then phage displaying Tat mutant peptide library were produced by infection of M13KO7 helper phage (Invitrogen Corp.).

Cell Panning The human keratinocyte cell line, HaCaT, was seeded in 6 well tissue culture plates at 5×10^5 cells/well

* To whom correspondence should be addressed. e-mail: tsunoda@nibio.go.jp
# These authors contributed equally to the work.

and cultured overnight. The culture medium was changed to Opti-Mem I medium (Invitrogen Corp.) containing 2% BSA for blocking and incubated for 2 h at 37 °C. Purified phage library was pre-incubated with the same medium at 4 °C for 1 h. The phage solution was then applied to the HaCaT cells and incubated for 2 h at 37 °C. Unbound phage was removed by extensive washing (20×) with PBS (pH 7.2). Phage particles bound or internalized with the HaCaT cells were subsequently rescued by adding ice cold 50 mM HCl to each well and incubating for 10 min at 4 °C. The solution containing lysed cells and phage library was collected and neutralized by adding 1.0 M Tris–HCl pH 8.0. The phage clones contained in the solution were propagated by infecting *E. coli* TG1 and applied for the next round of panning. The cell panning was repeated two more times (*i.e.* 3 panning rounds in total).

Expression of PTD-PSIF Proteins Protein synthesis inhibitory factor (PSIF, PE fragment) is an approximately 40 kDa fragment of the bacterial exotoxin (GenBank Accession No. K01397) derived from *Pseudomonas aeruginosa*[22] (ATCC strain No.29260). PSIF lacks its cell binding domain, and has been successfully used as a cytotoxic portion of a recombinant immunotoxin.[23] We cloned the cDNA for PSIF from *Pseudomonas aeruginosa*, Migula by PCR using the primer set: 5′-GAT GAT CGA TCG CGG CCG CAG GTG CGC CGG TGC CGT ATC CGG ATC CGC TGG AAC CGC GTG CCG CAG ACT ACA AAG ACG ACG ACG ACA AAC CCG AGG GCG GCA GCC TGG CCG CGC TGA CC-3′ and 5′-GAT CGA TCG ATC ACT AGT CTA CAG TTC GTC TTT CTT CAG GTC CTC GCG CGG CGG TTT GCC GGG-3′. The PCR product was cloned into modified pCANTAB phagemid vector. After 3 rounds of cell panning, the enriched library of PTD candidate cDNA clones were purified from phage-infected TG1 cells and inserted into the PSIF-fusion expression vector derived from phagemid pCANTAB5E. TG1 cells were transformed with the PTD-PSIF fusion library and monocloned. Transformed TG1 clones were picked, transferred to a 96 well plate format and cultured in 2-YT medium (Invitrogen Corp.) containing 2% glucose and 100 μg/ml ampicillin until the OD_{600} reached 0.5. PTD-PSIF protein was expressed in the supernatant by culturing the cells for 12 h at 37 °C in 2-YT growth medium with no glucose in the presence of 100 mM IPTG. These supernatants were harvested and used for the cellular cytotoxicity assay.

Cytotoxicity Assay of PTD-PSIF Fusion Protein against HaCaT Cells HaCaT cells were seeded on 96 well tissue culture plates at 1.5×10^4 cells/well in Opti-Mem I medium containing 50 μg/ml cycloheximide. Each culture supernatant from the PTD-PSIF clones was then added to an individual well. After incubation at 37 °C for 24 h, viability of HaCaT cells was assessed using the MTT assay.

Flow Cytometry Analysis of FITC-Labeled PTDs on Live Cells HaCaT cells were seeded on 24 well tissue culture plates at 1.0×10^5 cells/well. After incubation for 24 h at 37 °C, the cell monolayer was treated with FITC-labeled PTDs diluted in growth medium at a final concentration 10 μM for 3 h. Cells were then washed and any PTDs adsorbed to the cell surface digested using 2.5% trypsin. Cellular fluorescence was then measured by flow cytometry (Becton Dickinson, Oxford, U.K.).

***In Vitro* Safety Assessment** HaCaT cells were seeded on 96 well tissue culture plates at 1.6×10^4 cells/well. After incubation for 24 h at 37 °C, FITC-labeled PTDs were added to the cell monolayer at three different concentrations (3 μM, 10 μM or 30 μM). After additional incubation for 24 h at 37 °C, cell viability was assessed by the WST-8 assay (Dojindo Lab., Kumamoto, Japan).

Fluorescence Microscopic Analysis HeLa cells were seeded on a chamber coverglass at 3.0×10^4 cells/well in culture medium (MEM 10% fetal calf serum) and incubated for 24 h. A 2 μM aliquot of streptavidin modified Qdot525 (Quantum Dot Co., Hayward, CA U.S.A.) was incubated with 200 μM of synthesized biotinylated PTDs at room temperature for 5 min and diluted in culture medium containing 10% fetal calf serum (FCS) and 5 nM PTD-conjugated Qdot. HeLa cells were then treated with the culture medium containing PTD-Qdot and 100 ng/ml Hoechst 33342 (Invitrogen Corp.) and incubated at 37 °C for 1 h. The medium was then changed for Qdot-free medium and the cells observed by fluorescence microscopy using an Olympus IX-81 microscope (Olympus Co., Tokyo, Japan) at various time points.

RESULTS AND DISCUSSION

In this study, a screening method for Tat PTD mutants with efficient cell penetrating activity was established and novel peptide sequences were identified (Fig. 1). Mutagenic PCR, using primers Y-oligo22 3′ex and Tat[47—57]R), was used to prepare a mutant peptide gene library of Tat in which 5 codons were randomized within the Tat[47—57] peptide. All the natural arginine codons of this peptide were retained because arginine was reported to have an important roll for penetrating into the cells.[24] The PCR product was then ligated into the phagemid vector. Approximately 16 million colony forming units (cfu) were obtained after transformation of *E. coli* TG1 with the phagemid. DNA sequence analysis of the library confirmed it to be derived from independent clones (Table 1). Our results established that the library had an enormous repertoire covering the 3.2 million theoretical combinations of 5 amino acids. From this, a 1.0×10^{12}—10^{13} cfu phage library displaying Tat mutant was prepared. In order to enrich the phage clones which bound or internalized to the cells, 3 rounds of cell panning using the HaCaT cell line was performed. The enriched phage clones included not only PTDs capable of penetrating the cell but also those peptides which simply bind to the cell surface.

To allow the differential selection of PTDs capable of penetrating the cell we designed a high-throughput screening method by fusing PTD with PSIF. PSIF from *Pseudomonas aeruginosa*, was not by itself cytotoxic because the cell-binding domain was truncated. However, PSIF shows cytotoxicity when it is fused to a carrier, such as PTD, because it can then enter the cytoplasm.[21] PSIF-fusion is a simple and effective screening method for novel PTDs because the penetrating ability of the peptide can be evaluated from the cytotoxic effects of the fused protein. Figure 2A shows the cellular uptake of PTD-PSIF fusion from the Tat mutant library before cell panning. No clones displaying stronger cytotoxicity than wild-type Tat-PSIF fusion could be detected. However, after 3 rounds of cell panning, over 80% of the analyzed 800 clones showed stronger cytotoxicity than wild-type Tat-PSIF.

(Fig. 2B). Using this rapid PSIF screening method, we isolated superior PTD candidates in only 2—3 weeks. Clones showing enhanced cytotoxicity over wild-type Tat peptide were isolated and the DNA sequences analyzed.

Next, FITC labeled PTD mutant candidates were synthesized and cellular uptake was determined by flow cytometry (Fig. 3). Each of the PTD candidates displayed similar or increased uptake compared with wild-type Tat[47—57] or Tat[48—60]. In particular, cellular uptake efficiency of YM2 or YM3 was 2.5 to 3 fold greater than wild-type Tat. Table 2 shows the amino acid sequences of clones YM2 and YM3. Some clones, including YM2 or YM3, have an increased number of arginine residues (clones 1, 6 and 7, Table 1). Moreover, all the clones shown in Tables 1 and 2 have almost the same isoelectric point (pI) of *ca* 13. In general the transduction ability of PTDs is associated with cationic amino acid residues, such as arginine. However, our data indicates that the transduction ability of PTDs is not wholly dependent on the total number of arginine residues or the overall pI. Interestingly, YM2 and YM3 include some characteristic amino acid residues, such as proline. In addition, these PTD candidates have arginine at the same position as Tat 54, which is thought to be important for transduction. In this way, our phage display system can correlate the amino acid sequence of the peptides with transduction ability. Thus, for the first time, it may be possible to experimentally determine the factors that influence intracellular transduction other than cationic amino acids or pI.

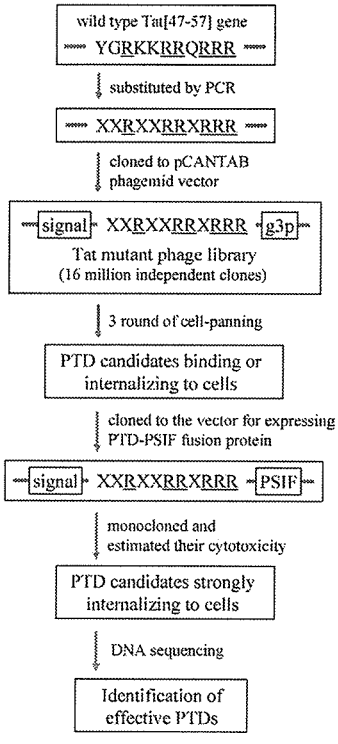

Fig. 1. Overview of the Creation of the Novel PTDs Using a Phage Display System Based High-Throughput Screening Method

The Tat mutant peptide gene library was constructed by randomization of the Tat[47—57] sequence, except for the arginine codons. Fixed arginine residues are underlined. Substituted amino acids are shown as X. After amplification, mutant Tat genes were cloned into pCANTAB phagemid vector. The Tat mutant phage library was produced from phagemid transformed TG1. The phage library was then subjected to 3 rounds of cell panning as described in Materials and Methods. Mutant Tat clones binding or internalizing to the cell were initially concentrated from the library. PTD candidates were then purified and cloned into PSIF expression vector. Monoclonal TG1s containing individual PTD-PSIF encoding phagemid were picked up separately into a 96 well format. The cytotoxicity of the PTD-PSIF proteins was assessed in order to isolate Tat peptide mutants that are strongly internalized within the cell. Approximately 1000 clones can be simultaneously assayed for cytotoxicity by this procedure. The amino acid sequence of effective Tat mutants were readily obtained from their DNA sequence.

To utilize PTD as an effective intracellular drug delivery carrier, the peptide must be nontoxic to the cells. Using the assay for HaCaT cells, no cytotoxicity was observed with peptides YM1, YM2 and YM3 (Fig. 4). Polyarginine is one of the representative artificial PTDs and, like Tat peptide, is highly efficient at transducing cargo into the cell.[24] However, polyarginine (Arg 11) displayed more cytotoxicity than Tat peptide.[25] Our initial assessment, conducted on a specific cell line, indicates that all 3 novel PTDs are safe drug carriers.

Another research group has also reported the generation of novel PTDs with enhanced transduction potential compared to that of Tat peptide.[14] However, it was never demonstrated whether these PTDs actually introduced cargos into the cell. Therefore, we examined whether our PTDs candidates were able to deliver macromolecules. Qdots, a fluorescent semiconductor nanocrystal, was used as a model macro drug molecule. Qdots streptavidin conjugate was modified with either biotinylated Tat[47—57] or YM3 peptide and then applied to cultured HeLa cells. After 1 h, Tat[47—57] or YM3 labeled Qdot were localized near the cell membrane (Figs. 5a, d). For these observations, Hela cell was used in spite of HaCaT cell because the localization analysis of Qdots in HaCaT cell was difficult due to its small cytoplasmic area. Upon further incubation, the location of the Qdot-PTD conjugates changed (Figs. 5b, e) until after 20 h the Qdot was observed at the perinuclear region (Figs. 5c, f). However, Qdots was not ob-

Table 1. Amino Acid Sequences and pI Values of Tat Mutants from the Library

Clone	Position											pI
	47	48	49	50	51	52	53	54	55	56	57	
Tat[47—57]	Y	G	R	K	K	R	R	Q	R	R	R	12.8
Clone1	T	L	R	T	R	R	R	N	R	R	R	13.3
Clone2	N	Y	R	T	G	R	R	K	R	R	R	12.8
Clone3	L	T	R	Q	T	R	R	M	R	R	R	13.2
Clone4	S	K	R	T	W	R	R	N	R	R	R	13.2
Clone5	K	E	R	H	L	R	R	H	R	R	R	12.8
Clone6	D	R	R	N	S	R	R	N	R	R	R	12.9
Clone7	H	R	R	P	V	R	R	F	R	R	R	13.3
Clone8	A	P	R	D	W	R	R	A	R	R	R	12.8

Sequence analysis of random phage clones isolated from the library. The library confirmed it to be derived from independent clones.

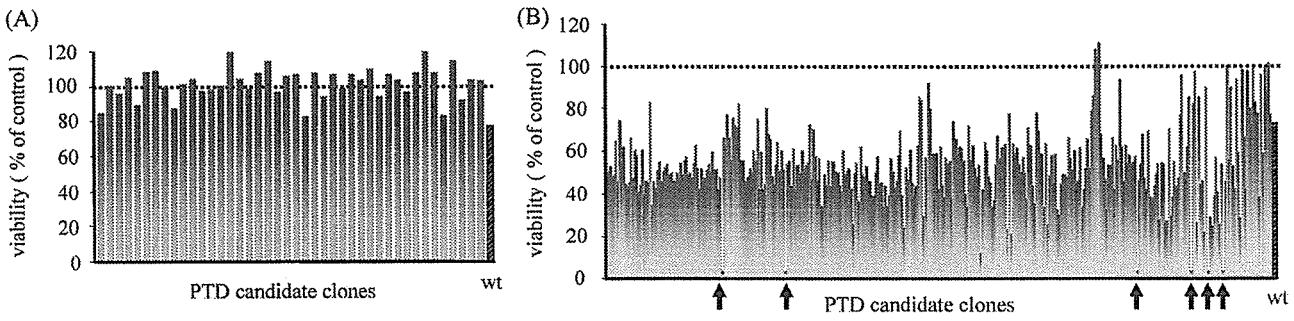

Fig. 2. Cellular Cytotoxicity Assay of the Monoclonal PTD Candidate-PSIF Fusion Proteins to HaCaT Cells

These figures show the cellular uptake of individual clones-PSIF fusion proteins from (A) Tat mutant library before cell panning and (B) concentrated novel PTD candidates after 3 rounds of cell panning. Cellular cytotoxicy was assessed using the MTT assay. The dose of PTD-PSIF fusion clones was adjusted to retain *ca.* 80% viability when using wild-type Tat-PSIF fusion protein (left stripy column). Clones in the arrowed columns showed greater cytotoxicity over wild-type Tat-PSIF fusion protein.

Table 2. Nucleotide and Amino Acid Sequences and pI Values of Novel PTDs

Clone	Position											pI
	47	48	49	50	51	52	53	54	55	56	57	
Tat[47—57]	Y	G	R	K	K	R	R	Q	R	R	R	12.8
	TAC	GGT	CGT	AAA	AAA	CGT	CGT	CAG	CGT	CGT	CGT	
YM1	R	N	R	A	R	R	R	Q	R	R	R	13.4
	AGG	AAC	CGT	GCC	CGC	CGT	CGT	CAG	CGT	CGT	CGT	
YM2	P	V	R	R	P	R	R	R	R	R	R	13.4
	CCC	GTG	CGT	CGC	CCC	CGT	CGT	CGG	CGT	CGT	CGT	
YM3	T	H	R	L	P	R	R	R	R	R	R	13.3
	ACC	CAC	CGT	TTG	CCC	CGT	CGT	CGC	CGT	CGT	CGT	

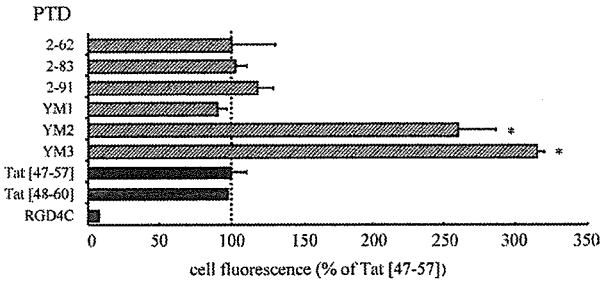

Fig. 3. Cellular Uptake of PTD-FITC Conjugates into HaCaT Cells

FITC labeled PTDs were incubated with HaCaT cell monolayer for 3 h and their cellular uptakes were estimated by flow cytometry analysis. Stripy columns show uptakes of PTD candidates from the Tat mutant library. Black columns show uptake of control PTDs. Control PTD sequences are as follows; Tat[47—57] (wild type Tat PTD): YGRKKRRQRRR, Tat[48—60]: GRKKRRQRRRPPQ, RGD4C: CDCRGDCFC. This experiment was performed at $n=3$. Each data value represents the mean±S.D. * $p<0.005$, compared with Tat[47—57].

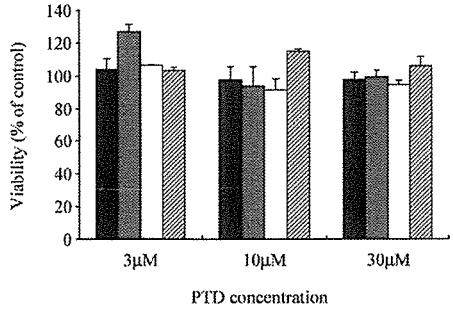

Fig. 4. *In Vitro* Safety Assessment of Tat Mutants

FITC labeled Tat[47—57] (■), YM1 (▩), YM2 (□) or YM3 (▨) were incubated with HaCaT cell monolayer for 24 h and their cytotoxicity was estimated using the MTT assay. Non-treated cells were arbitrarily given a value of 100%.

served in the cell nucleus. Recently, Tat peptides were reported to enter the cell by macropinocytosis.[26,27] By analogy, a large proportion of the incorporated Qdots may become trapped in the macropinosome and thus fail to transfer into the nucleus. Therefore, to achieve efficient drug delivery into the cytosol or organelles, the cargo must be released from the macropinosome. One possible strategy would be to incorporate the HA2 peptide to enhance the liberation of carrier and cargo protein from the endosome.[26,28]

It is reported that PTDs are able to deliver various bioactive molecules into cells. However their transduction efficiencies are not sufficient to achieve effective protein-based therapy. In this report, we used a high throughput screening method to successfully identify novel PTD mutants with improved cell penetrating activity over wild-type Tat peptide. The PTD mutants were found to contain some characteristic amino acids. These findings indicate that there may be many factors to account for cell penetration other than the presence of cationic amino acids. Using our high-throughput screening method, it should be possible to formulate some generic rules concerning the mechanism of cell penetration and subcellular transport. In conclusion, our high-throughput screening system is expected to contribute to the development of protein-based therapies.

Acknowledgments This study was supported in part by Grants-in-Aid for Scientific Research (No. 17689008, 17016084, 17790135, 18015055, 18659047) from the Ministry of Education, Culture, Sports, Science and Technology of Japan, in part by Health and Labor Sciences Research Grant from the Ministry of Health, Labor and Welfare of Japan, in part by Health Sciences Research Grants for Re-

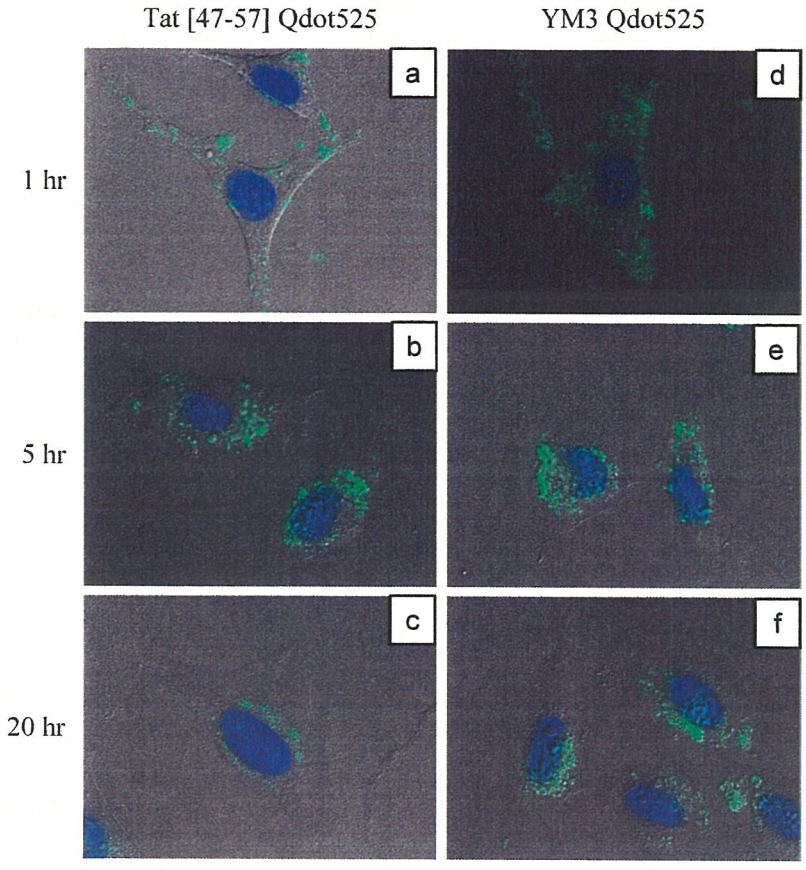

Fig. 5. Cellular Uptake and Intracellular Behavior of PTD-Qdot Complex in HeLa Cells

5 nM Tat[47—57] (a, b and c) or YM3 (d, e and f) labeled Qdots were incubated with HeLa cells. The cells were observed using fluorescence microscopy after 1 h (a and d), 5 h (b and e) or 20 h (c and f). The cell nucleus was stained with Hoechst 33342.

search on Health Sciences focusing on Drug Innovation from the Japan Health Sciences Foundation, in part by Takeda Science Foundation, in part by Industrial Technology Research Grant Program (No. 03A47016a) from New Energy and Industrial Technology Development Organization (NEDO), and in part by JSPS Research Fellowships for Young Scientists (No. 08476, 08841, 09131) from the Japan Society for the Promotion of Science.

REFERENCES

1) Wadia J. S., Dowdy S. F., *Curr. Protein Pept. Sci.*, **4**, 97—104 (2003).
2) Wadia J. S., Dowdy S. F., *Curr. Opin. Biotechnol.*, **13**, 52—56 (2002).
3) Prochiantz A., *Curr. Opin. Cell. Biol.*, **12**, 400—406 (2000).
4) Li Y., Rosal R. V., Brandt-Rauf P. W., Fine R. L., *Biochem. Biophys. Res. Commun.*, **298**, 439—449 (2002).
5) Cao G., Pei W., Ge H., Liang Q., Luo Y., Sharp F. R., Lu A., Ran R., Graham S. H., Chen J., *J. Neurosci.*, **22**, 5423—5431 (2002).
6) Shibagaki N., Udey M. C., *Eur. J. Immunol.*, **33**, 850—860 (2003).
7) Tanaka Y., Dowdy S. F., Linehan D. C., Eberlein T. J., Goedegebuure P. S., *J. Immunol.*, **170**, 1291—1298 (2003).
8) Kim T. G., Befus N., Langridge W. H., *Vaccine*, **22**, 431—438 (2004).
9) Tasciotti E., Zoppe M., Giacca M., *Cancer Gene Ther.*, **10**, 64—74 (2003).
10) Astriab-Fisher A., Sergueev D. S., Fisher M., Shaw B. R., Juliano R. L., *Biochem. Pharmacol.*, **60**, 83—90 (2000).
11) Lewin M., Carlesso N., Tung C. H., Tang X. W., Cory D., Scadden D. T., *Nat Biotechnol.*, **18**, 410—414 (2000).
12) Torchilin V. P., Rammohan R., Weissig V., Levchenko T. S., *Proc. Natl. Acad. Sci. U.S.A.*, **98**, 8786—8791 (2001).
13) Torchilin V. P., Levchenko T. S., *Curr. Protein Pept. Sci.*, **4**, 133—140 (2003).
14) Ho A., Schwarze S. R., Mermelstein S. J., Waksman G., Dowdy S. F., *Cancer Res.*, **61**, 474—477 (2001).
15) Morris M. C., Depollier J., Mery J., Heitz F., *Nat. Biotechnol.*, **19**, 1173—1176 (2001).
16) Yamamoto Y., Tsutsumi Y., Yoshioka Y., Nishibata T., Kobayashi K., Okamoto T., Mukai Y., Shimizu T., Nakagawa S., Nagata S., Mayumi T., *Nat. Biotechnol.*, **21**, 546—552 (2003).
17) Pasqualini R., Ruoslahti E., *Nature* (Lomdon), **380**, 364—366 (1996).
18) Pasqualini R., Ruoslahti E., *Mol. Psychiatry*, **1**, 421—422 (1996).
19) Smith G. P., *Science*, **228**, 1315—1317 (1985).
20) Rossenu S., Dewitte D., Vandekerckhove J., Ampe C., *J. Protein Chem.*, **16**, 499—503 (1997).
21) Kreitman R. J., *Curr. Opin. Immunol.*, **11**, 570—578 (1999).
22) Chaudhary V. K., FitzGerald D. J., Adhya S., Pastan I., *Proc. Natl. Acad. Sci. U.S.A.*, **84**, 4538—4542 (1987).
23) Kreitman R. J., Wilson W. H., Bergeron K., Raggio M., Stetler-Stevenson M., FitzGerald D. J., Pastan I., *N. Engl. J. Med.*, **345**, 241—247 (2001).
24) Futaki S., Suzuki T., Ohashi W., Yagami T., Tanaka S., Ueda K., Sugiura Y., *J. Biol. Chem.*, **276**, 5836—5840 (2001).
25) Jones S. W., Christison R., Bundell K., Voyce C. J., Brockbank S. M., Newham P., Lindsay M. A., *Br. J. Pharmacol.*, **145**, 1093—1102 (2005).
26) Wadia J. S., Stan R. V., Dowdy S. F., *Nat. Med.*, **10**, 310—315 (2004).
27) Kaplan I. M., Wadia J. S., Dowdy S. F., *J. Control. Release*, **102**, 247—253 (2005).
28) Michiue H., Tomizawa K., Wei F. Y., Matsushita M., Lu Y. F., Ichikawa T., Tamiya T., Date I., *J. Biol. Chem.*, **280**, 8285—8289 (2005).

Available online at www.sciencedirect.com
SCIENCE DIRECT®
Biochemical and Biophysical Research Communications 346 (2006) 198–204
BBRC
www.elsevier.com/locate/ybbrc

A novel method for construction of gene fragment library to searching epitopes

Maki Kawamura [a,b,1], Hiroko Shibata [a,b,1], Haruhiko Kamada [a,*], Takayuki Okamoto [b,1], Yohei Mukai [a,b], Toshiki Sugita [a,b], Yasuhiro Abe [a,b], Sunao Imai [a,b], Tetsuya Nomura [a,b], Kazuya Nagano [a,b], Tadanori Mayumi [c], Shinsaku Nakagawa [b], Yasuo Tsutsumi [a,b], Shin-ich Tsunoda [a]

[a] *Laboratory of Pharmaceutical Proteomics, National Institute of Biomedical Innovation, 7-6-8 Asagi, Saito, Ibaraki, Osaka 567-0085, Japan*
[b] *Department of Biopharmaceutics, Graduate School of Pharmaceutical Sciences, Osaka University, 1-6 Yamadaoka, Suita, Osaka 565-0871, Japan*
[c] *Department of Cell Therapeutics, Graduate School of Pharmaceutical Sciences, Kobe Gakuin University, 518 Arise, Ikawadani, Nishiku, Kobe 651-2180, Japan*

Received 14 May 2006
Available online 24 May 2006

Abstract

Identification of the epitope sequence or the functional domain of proteins is a laborious process but a necessary one for biochemical and immunological research. To achieve intensive and effective screening of these functional peptides in various molecules, we established a novel screening method using a phage library system that displays various lengths and parts of peptides derived from target protein. Applying this library for epitope mapping, epitope peptide was more efficiently identified from gene fragment library than conventional random peptide library. Our system may be a most powerful method for identifying functional peptides.

Keywords: Phage display system; Gene fragment library; Random peptide library; Epitope mapping; TNF-α

The ability to identify active core or epitope peptides from bioactive proteins is of considerable interest to many researchers. Active-center peptide and binding domain peptide of protein have been expected for target peptide, biological tool, and more reasonable medicine, such as RGD peptide [1], Tat peptide [2], and Angiostatin/Endostatin [3,4]. On the other hand, applications of epitope peptide for anti-viral, cancer, and allergy immunotherapy have been extensively tried [5–8]. One of the most effective and frequently used methods for searching and identifying these functional peptides is phage display technology. Phage library which involves the expression of random peptides on its envelope as a fusion protein has been commonly used for this purpose [9–11]. But screening of target peptide from random peptide library is not effective, because theoretical diversity of random peptide library is enormous. For example, while the theoretical diversity of 10 mer random peptide library is 10 trillion (20^{10}), the maximum diversity is actually 10 million (1/1000 of theoretical size). Thus construction of gene fragment library which expresses random fragments of cDNA on phage particles has been tried [12–14]. Unlike random peptide library, gene fragment library is usually constructed for each target protein and supposed to be quite effective at much lower library sizes. If the length of target protein is 200 amino acids, the theoretical diversity is 2 million. However, conventional method for gene fragment library has the following limitations: (1) the gene fragmentation process with DNase is incomplete, resulting in poor variety of the fragment library; (2) with the use of blunt-ended insert DNA,

* Corresponding author. Fax: +81 72 641 9814.
E-mail address: kamada@nibio.go.jp (H. Kamada).
[1] These authors contributed equally to the work.

0006-291X/$ - see front matter © 2006 Elsevier Inc. All rights reserved.
doi:10.1016/j.bbrc.2006.05.103

unidirectional cloning cannot execute; (3) translational frame shift cannot be prevented. Therefore, this conventional phage library method is extremely limited for isolating functional peptide fragments. We therefore improved the technique and established a novel library system which enabled construction of a gene fragment library covering all regions and various lengths of the target protein.

Materials and methods

Reagents. Reagents for transcription were from Promega (Madison, WI), and T7 RNA polymerase was from TAKARA BIO (Shiga, Japan). Smart Race cDNA Amplification Kit was from Clontech Laboratories (Mountain View, CA). Other reagents for reverse transcription were from Invitrogen (Tokyo, Japan). 5′-RACE PCR was performed by Advantage-HF2 PCR kit (Clontech Laboratories, Inc.). Accu Taq LA DNA polymerase (Sigma–Aldrich Japan, Tokyo, Japan) was used for nested PCR. DNA and RNA were purified with QIAquick PCR Purification Kit and RNeasy mini kit (QIAGEN, Valencia, CA), respectively. *Escherichia coli* TG1 was purchased from STRATAGENE (Tokyo, Japan). Anti-FLAG monoclonal antibody was from Sigma–Aldrich. Rabbit anti-human TNF-α polyclonal antibody was from CALBIOCHEM (Darmstadt, Germany). Mouse anti-M13 phage-horseradish peroxidase (HRP) conjugate and pCANTAB5E were from Amersham–Pharmacia Biotech (Uppsala, Sweden).

Construction of gene fragment library. Fig. 1 is a flow diagram that shows the construction of gene fragment library. TNF-α coding target region, domain 1, 2, and 3 were amplified and T7 promoter was added at the 5′ end by PCR. PCR products were transcribed with T7 RNA polymerase at 37 °C for 2 h, yielding sense RNA of only the target region. The RNA samples were reverse transcribed with the Smart Race cDNA Amplification Kit using random nonamer primers that contained *Mro*I site at the 5′ end. In this reaction, after reverse transcriptase reaches the ends of the mRNA template, it adds several dC residues to synthesized cDNA. The adaptor oligonucleotide anneals to the tail of the cDNA and serves as an extended template for reverse transcriptase. Following reverse transcription, the first-strand cDNA was used directly in 5′-RACE PCR using synthetic primers, which anneal to the adaptor oligonucleotides and *Mro*I site, respectively. The condition of 5′-RACE PCR was cycled 5 times at 94 °C for 30 s, 72 °C for 3 180 s, 5 times at 94 °C for 30 s, at 70 °C for 30 s, and at 72 °C for 180 s, and 20 times at 94 °C for 30 s, at 68 °C for 30 s, at 72 °C for 180 s. Consequently, dsDNA was obtained, which contains T7 promoter and *Mro*I site, and begins randomly at the 5′ end. After the cDNA was transcribed with T7 RNA polymerase, mRNA was reverse transcribed by Super Script III using random nonamer containing the *Nco*I site to yield single strand DNA that began randomly at the 3′ end of the sense strand. The gene library was amplified by PCR and constructed with *Nco*I site at the 5′ end and *Mro*I site at the 3′ end, and coded various range of TNF-α. PCR was cycled 35 times at 96 °C for 60 s, at 59 °C for 60 s, and at 68 °C for 60 s. The gene library was then digested with *Nco*I and *Mro*I was ligated with the phagemid vector pY03-FLAG (*Mro*I) to display TNF-α fragments on the phage surface as fusion proteins with g3p. pY03-FLAG (*Mro*I) was constructed by inserting the *Mro*I and FLAG sequence between E tag and g3p gene of pCANTAB 5E. The phage library was prepared as described [15].

Selection of phages displaying FLAG tag. Ten micrograms per milliliter of Anti-FLAG monoclonal antibody was coated onto Maxisorb immunotubes (NUNC). After blocking, TNF-α gene fragment phage library was then added into the anti-FLAG antibody-coated immunotubes and incubated for 1 h at 4 °C. Random 18 mer peptide phage library was constructed by almost the same method as previously described [16] and used as a control. After washing the tubes with PBS containing 0.05% Tween 20, the bound phages were eluted by incubating the tubes with 100 mM HCl. Eluted phages were immediately neutralized with 1 M Tris–HCl and then added to log phase *E. coli* TG1 cells. For panning of the anti-TNF-α antibody, the infected TG1 cells were grown to log phase, rescued with M13KO7 helper phage, and purified by polyethylene glycol (PEG) 6000/NaCl precipitation.

Selection of phages displaying peptide bound to anti-TNF-α antibody. Ten micrograms per milliliter of rabbit anti-TNF-α polyclonal antibody was coated onto 96-well immune plate (NUNC). The procedures were followed as mentioned above (the section of "*Selection of phages displaying FLAG tag*"). After the third round of panning, eluted phages in each round of panning were used for phage ELISA to estimate the number.

Phage ELISA. For measurement of output/input ratio, the eluted phages were added to 96-well immune plate coated with each antibody and incubated at RT for 2 h. The plates were washed three times with PBS and 0.05% Tween PBS, and incubated with anti-M13 phage-horseradish peroxidase (HRP) conjugate for 1 h. After incubation, the plates were washed three times, TMB peroxidase substrate (Nacalai Tesque, Kyoto, Japan) was added, and the absorbance was read at 450 nm using a microplate reader. To assess affinities of individual phage clones, infected TG1 cells were isolated, grown at 37 °C in 96-well plate, and rescued with M13KO7 helper phage. Amplified phage particles were added to anti-TNF antibody coated plate and following the above procedure.

Peptide ELISA. Biotinylated epitope peptide was used for binding analysis. Mab1-peptide, Mab4-peptide, and 3D6-peptide were used for control peptides. Each peptide corresponds in position to a.a. 127–137, a.a. 34–45, and a.a. 22–33 of TNF-α, respectively. Peptides were added to 96-well immune plate coated with the anti-TNF antibody and detected by Streptavidin HRP conjugate. The following procedure was performed as described in the above section.

Results

Library construction

We used human tumor necrosis factor-α (TNF-α) as a model protein to confirm the usefulness of our method. One area of improvement was that we could generate gene fragments with the *Sfi*I site at the 5′ end and *Mro*I site at the 3′ end, in the same orientation as the original gene, by using unidirectional reverse transcription and amplification of mRNA by T7 RNA polymerase [17]. Three TNF-α gene fragment libraries were constructed using TNF-α cDNA divided into 3 domains (domain 1, a.a. 1–85; domain 2, a.a. 40–123; and domain 3, a.a. 75–157) as a template. This library theoretically contains all TNF-α peptide sequences of less than 46 a.a. The TNF-α fragment library was produced by the procedure shown in Fig. 1. The number of the independent clones was 2.0×10^7 CFU, containing from domain 1, 7.1×10^6 CFU; domain 2, 5.6×10^6 CFU; and, domain 3, 7.3×10^6 CFU. The repertoire of the library sufficiently exceeded the theoretical variety for a fragment peptide library from 3 domains (8.2×10^3 CFU). The sequences of clones from this library were randomly analyzed (Fig. 2). Although gene fragments from domain 2 and 3 library tended to be located nearer the 5′ end of each domain, gene fragments from domain 1 were originated from various lengths and parts of the TNF-α sequence. All of the gene fragments had the assumed orientation. Thus we have some success in the creation of a library composed of fragments of various lengths and parts of TNF-α. However, the library was initially contaminated by unexpected clones whose lengths of the insert gene that were not multiples of 3, resulting in

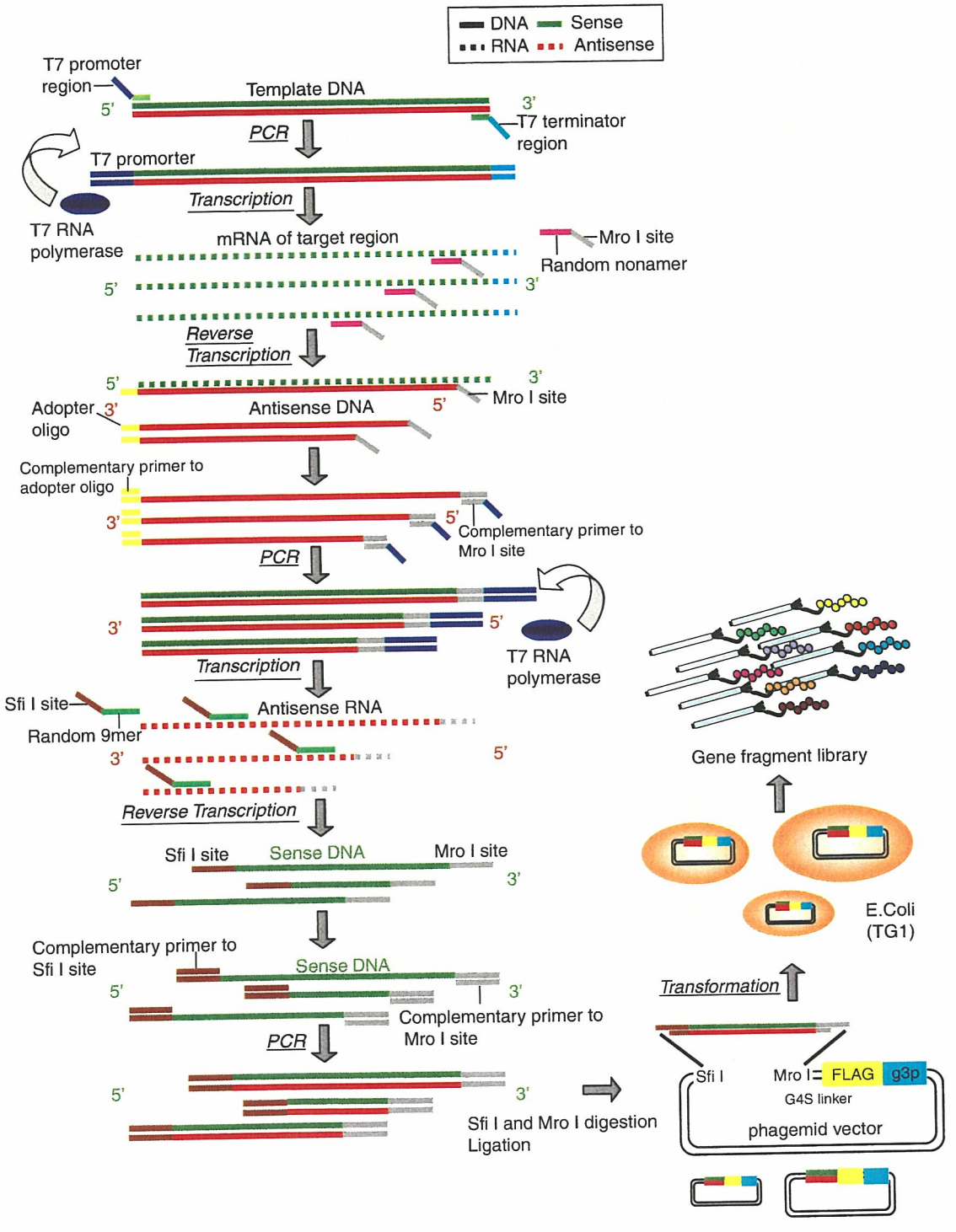

Fig. 1. Scheme for construction of a novel gene fragment library.

frame shifts. These clones cannot express target peptide as a fusion protein with envelope g3p and FLAG peptide, which develops downstream. Phage clones that did not express fragments of TNF-α and g3p as a fusion protein were removed with FLAG tag, which was inserted between the DNA coding fragment peptide by using anti-FLAG antibody. We were thus able to create a library that covered TNF-α fragments of various lengths and regions.

Affinity selection with anti-TNF-α antibody

To assess whether a specific peptide could be selected from this library, epitope mapping of a rabbit anti-TNF-α polyclonal antibody was performed. The number of phage clones expressing peptides that bind to anti-TNF-α antibody was estimated by measuring the output phages after each panning round using anti-TNF-α and

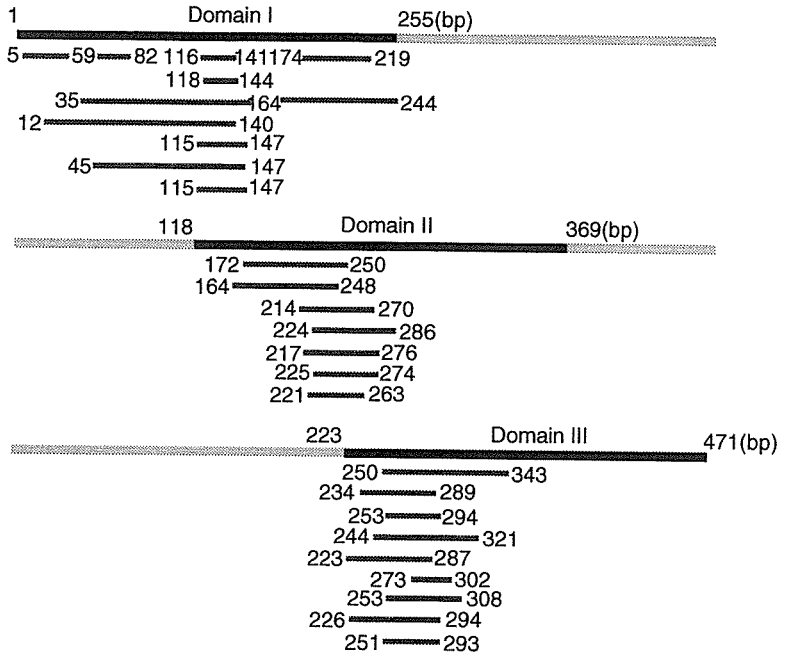

Fig. 2. Schematic representation of nucleotide sequences of peptides selected from the TNF-α gene fragment library.

anti-FLAG antibody (Fig. 3). Consequently, the output/input ratio of phage clones bound to anti-TNF-α antibody increased with each panning round, suggesting that the phage which expresses the peptide bound to the antibody was enriched. In contrast, when a random peptide library was used as a control, the number of control phage clones did not increase even after the second panning round. These results suggested that target peptides can be selected more effectively using our gene fragment library than with a conventional random peptide library.

Individual clones were isolated from output phages after each panning round and ELISA was performed to select clones that bound to anti-TNF-α antibody. Many clones had strong affinity for the antibody after the second panning, whereas almost none of the clones did prior to panning (Fig. 4). In addition, similar results were observed using other clones of anti-TNF-α antibodies (data not shown). In order to identify the peptide containing the epitope, we analyzed the insert sequences of phage clones which bound strongly to the antibody. Unexpectedly, we obtained phage clones which displayed peptides that contained amino acid 15–33 sequence of TNF-α (Fig. 5). Thus, this TNF-α fragment peptide was chemically synthesized as an epitope peptide and assessed its affinity for anti-TNF-α

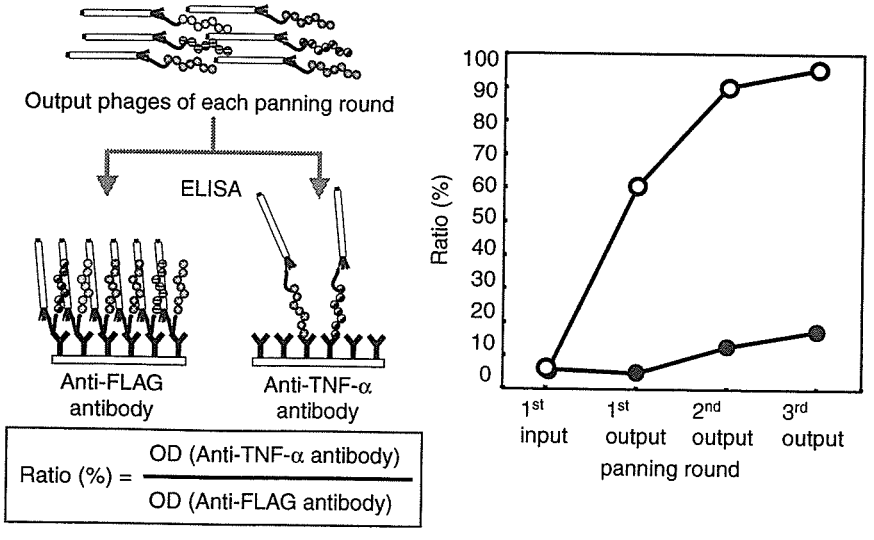

Fig. 3. Selection of phage clones expressing peptides binding to anti-TNF-α antibody. TNF-α gene fragment library (○) and the random 18 mer peptide library (●) were applied to immunotubes with immobilized anti-FLAG antibody or anti-TNF-α polyclonal antibody. Phage clones bound to each antibody were then selected as described in Materials and methods.